UNIVERSITÀ
DEGLI STUDI
DI BRESCIA

DOTTORATO DI RICERCA IN

PRECISION MEDICINE

BIO/13

CICLO

XXXVI

Characterization of the crosstalk between immune and Head and Neck cancer cells using the 3D collagen-base scaffold system to mimic the ECM

DOTTORANDO

Giacomo Miserocchi

NOME DEL SUPERVISORE

Prof. Marco Schiavone

NOME DEL Co SUPERVISORE

Dott.ssa Laura Mercatali

Abstract

Introduzione

I carcinomi a cellule squamose del distretto testa collo (HNSCCs) sono un gruppo di tumori che si originano dalle cellule squamose epiteliali delle relative sedi anatomiche. La loro crescente incidenza richiede consapevolezza, diagnosi precoce e migliori approcci terapeutici. Il microambiente tumorale ha dimostrato di avere un'importante influenza sui processi e l'andamento tumorale e questi effetti biologici vengono mediati non solo dalle cellule tumorali ma anche dalle componenti infiltrative e dalla matrice extracellulare. I monociti rappresentano la frazione circolante più numerosa della componente immunitaria innata e diversi studi hanno descritto questa popolazione come un'importante regolatore dei processi tumorali.

La mancanza di modelli in vitro affidabili di HNSCCS che riproducano l'eterogeneità del microambiente tumorale e della struttura della matrice extracellulare rappresenta un limite per gli studi traslazionali. L'ottimizzazione di sistemi di colture basate su scaffold hanno aumentato l'affidabilità del in vitro di mimare gli stimoli bio-strutturali del tessuto naturale. Qui proponiamo uno scaffold tridimensionale basato sul collagene che mimi il microambiente tumorale ed il crosstalk tra cellule tumorali, matrice extracellulare e monociti

Materiali e Metodi

Le fasi iniziali di questo progetto consistono nella sintesi degli scaffold in collagene e nella caratterizzazione di monocolture (monociti e cellule di HNSCC) e co-colture. La concentrazione di semina delle cellule ed il terreno ottimale sono state determinate sia per il modello 2D che per quello 3D. Per determinare la vitalità cellulare è stato utilizzato il test dell'MTT. Le differenti dinamiche di crescita nel core e nella periferia dello scaffold sono state valutate utilizzando un indicatore fluorescente del ciclo cellulare. L'influenza delle cellule tumorale e della struttura 3D sulla polarizzazione dei monociti è stata studiata mediante citofluorimetria.

Risultati e conclusioni

I risultati ottenuti ci hanno permesso di caratterizzare un nuovo modello in vitro per studiare il cross-talk che si sviluppa tra cellule tumorali e monociti in un microambiente tumorale. Abbiamo accuratamente selezionato le concentrazioni di cellule seminate ed i terreni di coltura ottimali per la crescita dei monociti e delle cellule tumorali nello scaffold in collagene. Da un punto di vista spaziale, la periferia del device induce una più alta proporzione di cellule proliferanti rispetto alle regioni interne, ricapitolando la struttura tissutale tipica delle masse tumorali organizzate in un core necrotico circondato da popolazioni cellulati proliferanti. Le analisi al citofluorimetro hanno evidenziato la capacità della struttura 3D di influenzare la polarizzazione dei monociti in macrofagi M2 attraverso l'espressione di markers pro-infiammatori. In più, le cocolture erano capaci di promuovere differenti tipi di polarizzazione dei monociti in base alla linea tumorale cellulare utilizzata. Tutti questi risultati fanno del nostro device 3D biomimetico un promettente strumento per aumentare l'affidabilità degli studi in vitro sulle interazioni delle cellule tumorali con la matrice extracellulare ed il sistema immunitario.

Abstract

Introduction

Head and neck squamous cell carcinoma (HNSCC) are a heterogeneous group of malignancies originating in the squamous epithelial cells of head and neck anatomical regions. Their increasing incidence calls for awareness, early detection, and improved therapeutic approaches. Tumor microenvironment (TME) has an important influence on tumor processes and behaviors, and these biological effects are mediated not only by tumor cells but also by infiltrating cell components, and extracellular matrix (ECM). Monocytes represent the major circulating cellular fraction of innate immune cell components, and different studies have described this cell population as an important regulator of cancer processes.

The lack of reliable HNSCC in vitro models mimicking the heterogeneity of TME and ECM structure represents a barrier for translational studies. The optimization of scaffold-based culture systems has increased the in vitro reliability to mimic the bio-mechanical stimuli of natural tissues. We propose a 3D biomimetic collagen-based scaffold to mimic the tumor microenvironment and the crosstalk between cancer cells, extracellular matrix (ECM), and monocytes.

Materials and methods

The initial steps of the project involved the synthesis of collagen-based scaffolds and a comprehensive characterization of cell monocultures (monocytes and HNSCC cells) and co-cultures. The optimal cell-seeding concentrations and culture media determined in both 2D and 3D models. MTT assays were performed to determine cell viability. The different cell growth dynamics in the 3D core and edge area were evaluated using fluorescence ubiquitination-based cell cycle indicator. The influence of tumor cells and 3D structure on monocytes polarization was studied through cytofluorimetric analysis.

Results and conclusions

The results obtained have enabled us to characterize a new model to study the crosstalk between tumor cells and monocytes in a 3D microenvironment. We have carefully selected the optimal cell-seeding concentrations and the best culture media for the growth of monocytes and HNSCC cells in the collagen-based scaffold structure. By a spatial point of view, the peripherical zone of the device showed a higher proportion of proliferative cells respect to the inner area, recapitulating the tissue structure typical of the tumor mass organized in a necrotic core covered by proliferative cell populations. The cytofluorimetric analysis highlighted the capability of the 3D structure to induce the polarization of monocytes to M2 macrophages through the expression of pro-inflammatory markers. Moreover, co-cultures were able to promote different kind of monocytes polarizations depending on the HNSCC cancer cell line used. All these results make our biomimetic 3D device a promising tool to increase the reliability of in vitro studies on the interaction between ECM, immune and cancer cells.

Index

1. Introduction

Head and neck cancers (HNC) represent the sixth most common non-skin tumor worldwide, causing about 450.000 new deaths and about 890.000 new cases every year [1]. More than 90% of total HNCs are squamous cell carcinomas (SCCs) of epithelial origin [2]. These cancers arise in the squamous epithelial cells of the oral mucosa, paranasal sinuses, larynx, oropharynx, hypopharynx, nasopharyngeal, and salivary glands [3]. HNSCCs management resents significant challenges in terms of treatments, diagnosis, patient outcomes, making these cancers a major public health concern worldwide. Given their complex nature, HNSCCs require a multidisciplinary and comprehensive clinical approach to effectively face their heterogenic features and improve patient prognosis. Clinicians evaluate several parameters before the therapy selection, including tumor site, stage, and patients' phenotype. The high cost and the severe side effects of anticancer agents make the identification of predictive and prognostic markers a priority for the stratification of responder and non- responder patients. The current clinical approaches include chemotherapy, immunotherapy, surgery and radiotherapy, treatments often aggressive and carrying considerable side effects [4,5]. Moreover, present treatments lead to poor prognostic outcomes and only 40%-50% patients survive more than 5 years although, during the last decades, there has been a modest improvement in the HNSCC survival rate, rising from 55% between 1992 and 1996 to 66% between 2002 and 2006 [6]. Precision medicine represents an innovative therapeutic strategy that aims at disease prevention and tailored treatments through comprehensive analysis of patients' individual genome, pathophysiological tumor features and lifestyle. Due to the heterogenic features and unpredictable clinical outcomes of these diseases, precision medicine represents a new hope for HNSCC patients.

1.1 HNSCC Epidemiology

According to the Global Cancer Observatory (GLOBOCAN) data, HNSCC represents a growing public health concern, with an estimated incidence of 1.08 million new cases yearly by 2030 [7]. The prevalence of HNSCC varies across the different world areas, with Australia and Southeast Asia showing high rates attributed to the lifestyle, such as alcohol and tobacco abuse, and environment [6,7]. In contrast, Western Europe and United States are experiencing an increased incidence of HNSCC cases due to the growth of human papillomavirus (HPV) infection rate [6]. Indeed, HNSCC has two primary etiological factors: the alcohol and smoking abuse, and specific viral infections [8,9]. HPV and Epstein-Barr virus (EBV) represent viral infection associated to the onset of HNSCCs. HPV-positive HNSCCs mainly arise in the oral cavity and oropharyngeal tissues while, EBV-related cancers are normally associated to the nasopharyngeal site especially in east and Southeast Asia, where this kind of tumor is endemic. HPV-related tumors typically affect patients at younger ages (between 50 and 53 years) if compared to HPV-negative HNSCC, where the median age of diagnosis is

66 years [10]. Men face a significantly higher risk (two- to four-fold) of developing HNSCC compared to women. The higher male to female ratio in HPV-negative HNSCC cases is consistent with sex-specific patterns of modifiable risk behaviors, such as alcohol consumption, tobacco use, areca nut chewing, and betel quid consumption [6,8]. Other risk factors for HNSCC include age, poor oral hygiene, exposure to carcinogenic air pollution, and a diet lacking in vegetables [6]. Moreover, the survival rates vary based on the HPV status of the tumor, with HPV-positive HNSCC patients showing better outcomes than those with HPV-negative tumors. This observation is supported by the Surveillance, Epidemiology, and End Results (SEER) program analysis, which includes tissue testing for HPV [11]. As the incidence of HNSCC continues to rise and its etiological factors evolve, ongoing research and advancements in early detection and targeted therapies will be crucial in effectively managing this complex disease and improving patient outcomes. Understanding the interplay between viral infections and HNSCC development will guide the implementation of preventive measures, such as vaccination programs, to mitigate the impact of these risk factors on the global burden of HNSCC.

1.2 HNSCC clinical approaches

Due to the high heterogeneity of this group of malignancies, the personalized therapeutic approach seems to be necessary to increase the efficacy of patients' treatment. Indeed, several parameters have to be evaluated before the therapy selection, such as tumor stage, site, biological and genetic features and clinical status [12]. Preservation of the organ's function is one of the first aims of an effective treatment. In local or loco-regional settings, the main clinical approaches are represented by surgery, chemotherapy and radiotherapy [13,14]. Oral cavity SCCs are commonly resected as first therapeutic option while other sites, such as larynx and pharynx, are cured with standard or hypo-fractionated radiation [15]. The use of laser or robotic resection technologies, combined with reconstructive techniques, represent minimal invasive approaches and allow the preservation of tissue integrity, especially in laryngeal tissues [16]. In order to prevent tumor relapse and to improve the patients' survival, lesions at high risk of recurrence are normally treated with chemoradiotherapy (CRT), with high doses of cisplatin-based chemotherapy and radiotherapy, or postoperative radiation [14,17]. These kinds of malignancies are characterized by extra-nodal extension, surgical margin involvement and perineural invasion. The first chemotherapeutic approach used for the treatment of HNSCCs is based on high dose cisplatin-based monotherapy (100 mg/m^2) or lower doses in cases presenting hearing loss or renal dysfunctions [18]. The combination of different anticancer agents represents one treatment strategy in recurrent or metastatic setting [19,20]. Targeted therapies are other curative options employed in the management of HNC patients. One example is represented by cetuximab, an epithelial growth factor receptor (EGFR) monoclonal antibody that was demonstrated to increase the

radiotherapy efficacy [18]. In this scenario, clinical and preclinical research need to identify new treatment approaches.

In the last decade, immunotherapy (IT) has been tested as an innovative therapeutic strategy for the treatment of HNSCCs. The “cancer immunosurveillance” theory, developed by Lewis Thomas and Sir Frank Macfarlane Burnet, suggests the immune system implication in recognizing and attacking of tumor-associated neoantigens in order to prevent cancer formation [21]. This theory gained support from clinical cases of spontaneous melanoma regression in individuals with autoimmune diseases and successful immune responses after tumor adoptive transfer in mice. The discovery of tumor-specific immune responses revolutionized oncology, extending survival for otherwise rapidly fatal tumors [22]. Immunotherapy is now a frontline treatment for many cancer types, and its role is expected to grow further with the discovery of new treatment approaches and druggable targets. Immunotherapeutic drugs perform their anti-cancer effect through the activation of patient’s immune system. Unlike other cancer treatments, immunotherapy does not directly attack the tumor but focuses on enhancing the body's natural defense mechanisms against cancer [23]. Key immunological checkpoint molecules in T cells are represented by the Programmed cell death 1 (PD1) and cytotoxic T lymphocyte antigen 4 (CTLA4), two proteins that are responsible of the self-tolerance maintaining and protect against infections and neoplasia [24]. Preclinical research has explored the potential of PD1 axis inhibitors in cancer treatment and identified new biomarkers. Inhibition of the PD1 axis was found to enhance CD8+ T cell cytotoxic antitumor responses by reversing the constraining effects of PDL1 or PDL2 overexpression in cancer cells and promoting tumor rejection in mice lacking functional PD1 [24]. In 2016, it was approved the use of two anti-PD-1 monoclonal antibodies, pembrolizumab and nivolumab, for the treatment of metastatic or recurrent HNSCCs based on the results of phase III clinical trials, demonstrating the effectiveness of mAbs targeting the detrimental immunoregulatory effects of the PD1 axis [25]. For patients with PDL1-expressing tumors or microsatellite instability, pembrolizumab, a humanized anti-PD1 IgG4 antibody, is recommended as part of their systemic treatment [26]. Hyper-progression is a common result of immune checkpoint inhibition therapies in HNSCC patients, particularly in cases of local or regional recurrence, HPV-negative cancer, and when immunotherapy is selected instead of chemotherapy [27]. Close monitoring and quick treatment adjustments are essential requirements to improve the disease management. Nowadays, clinical trials are exploring new immunotherapeutic approaches, including combinations of immune checkpoint inhibitors and multi-targeted kinase inhibitors or anti-angiogenic agents, for the treatment of metastatic and/or recurrent HNSCC [19].

1.3 Carcinogenesis of HNSCCs

Genetic mutations, viral infection, alcohol and tobacco abuse are the major risk factors of HNSCCs occurrence. Carcinogenesis represents a series of sequential pathological steps involving different cell

populations. The development of HNSSCs are driven by epithelial cells' hyperplasia that results in mild, moderate or severe dysplasia [6]. HNSCC has two primary carcinogenic processes, induced by chromosomal instability and gene mutations that are induced or independent by viral infection. Notably, the consumption of carcinogens from tobacco and excessive alcohol intake, both independently and combined, is strongly associated with an increased risk of developing HPV-negative HNSCCs. Additionally, specific oncogenic strains of the human papillomavirus (HPV), particularly HPV-16 and HPV-18, are frequently detected in cases of oropharyngeal tumors HNSCCs (Figure 1) [28].

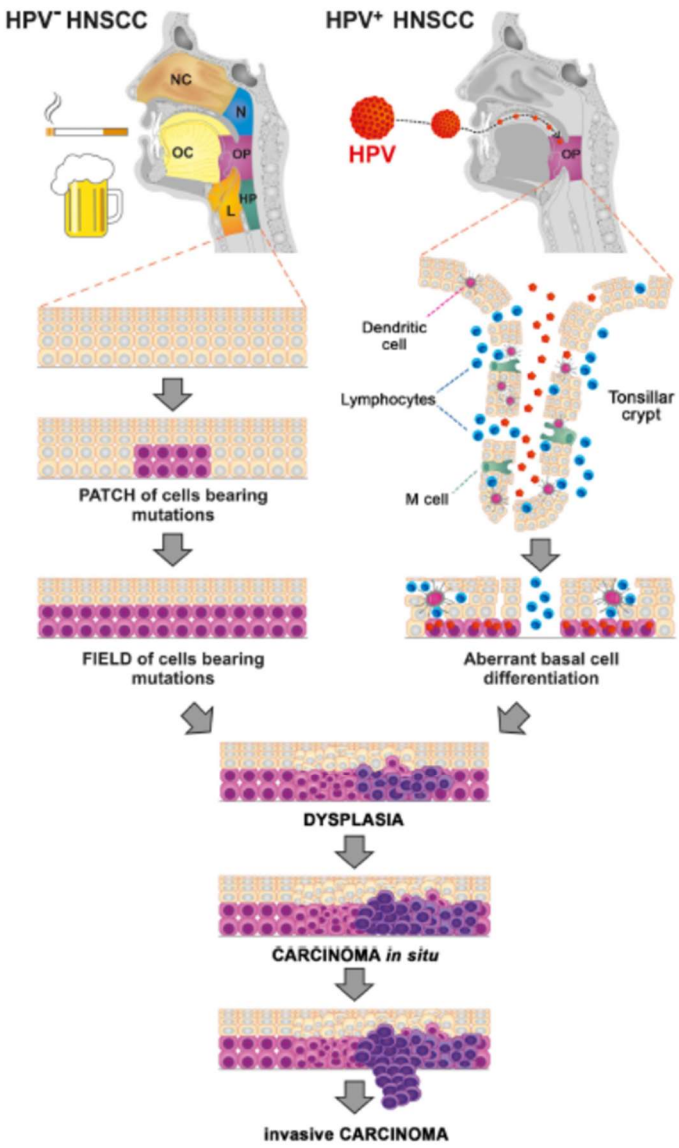

Figure 1: Carcinogenesis process in HPV negative and HPV positive HNSCCs [28].

The malignant progression to neoplasia can be induced by different kind of cells, a feature associated to the heterogeneous nature of these tumors. In this context, the oncogenic processes are mainly driven by the transformation of either progenitor cells or adult stem cells into cancer stem cells (CSCs) [29]. CSCs are a

minority subpopulation of all tumor subclones characterized by self-renewal properties and the capability to differentiate into progeny with transient proliferative status [30]. CSCs express specific markers in numerous solid tumors, such as aldehyde dehydrogenase (ALDH), an enzyme involved in the oxidation of aldehydes to carbolic acid, and the cell adhesion molecule CD44. In HNSCCs, the CSCs number and plasticity are related to the HPV status [31,32]. Even though CSCs represent a small fraction of all tumor cells, their self-renewal properties are one of the causes of resistance to standard therapies [33]. For these reasons, CSCs are studied as promising target for innovative therapies and a source of biomarkers of chemo- and radio-resistance to stratify the patients for personalized therapies [29,33]. Chromatin regulator Bmi-1 and CD133 are two examples of CSCs markers related to drug resistance but their expression is not HPV dependent [34-36] while, radio-resistance processes are related to the high efficacy of this kind of cells to repair the DNA damage.

When HNSCC positive and negative for HPV were compared, no significant changes in overall mutation rates were found. The most common genetic alterations associated to HPV-negative onset are represented by loss of CDKN2A, amplification of CCND1 and mutations in TP53, FAT1, NOTCH and PIK3CA [37,38]. Tobacco abuse constitutes the main risk factor of HPV-negative HNSCCs onset. Cigarettes contain more than 5,000 compounds, including nitrosamines and polycyclic aromatic hydrocarbons (PAHs), compounds considered one of the main carcinogens found in tobacco [39]. The metabolically activated carcinogens from tobacco, such as PAHs and nitrosamines, can lead to the formation of covalent DNA adducts. These adducts have the potential to cause mutations and other genetic disorders, contributing to the neoplastic transformation seen in head and neck squamous cell carcinoma (HNSCC) and other cancers. In addition to the direct carcinogenic effects, the smoking of tobacco is also associated to the activation of inflammation process, which plays a crucial role in angiogenesis, proliferation, and carcinogenesis.

HPV-positive HNSCCs display a different mutation pattern respect to the HPV-negative counterparts. The main genetic alterations include loss of TRAF3, amplification of E2F1, and PIK3CA mutations [37,38]. The 70% of these tumors arise in oropharynx [40]. Among all the HPV types, HPV-16 is the most widespread virus strain associated to HNSCC occurrence. Among the nine proteins encoded from the viral genome, E6 and E7 are the main actors implicated in the malignant transformation [41]. E6 is able to produce complexes with the tumor suppressor P53, inducing ubiquitylation and subsequent proteasomal degradation [6,41]. The activity of P53 is altered also in HPV-negative tumors but it depends on the inactivation of the enzyme due to the deletions or mutations of TP53 gene [42,43]. Moreover, E7 promotes proteasomal degradation of retinoblastoma-associated protein (Rb1), a cell cycle regulator [43]. The lower level of Rb1 induces the cell cycle progression through the upregulation of p16, an inhibitor of cyclin-dependent kinases (CDK) and a diagnostic marker of HPV-positive HNSCCs [43,44]. Inactivation of p53 and Rb1 disrupts the cell cycle control, leading to uncontrolled cell proliferation and contributes to the tumor progression.

One of the last steps of carcinogenesis is represented by the evasion of the immune surveillance. Indeed, CSCs establish a crosstalk with immune cells populations that promote an immunosuppressive milieu that induce the tumor progression as a result of escape from the patients' immune surveillance [45-47]. In this scenario, the study of the evasion and dysregulation of the immune system activity in the pathogenesis of HNSCCs provides the basis for the improvement of therapeutic approaches and patients outcomes.

1.4 Tumor microenvironment

Cancers are represented by a pool of several malignant subclones continuously cross-talking with other cell populations and tissues to promote the tumor proliferation and dissemination. In this context, the development of the lesions alters the tissue physiology and cells genotype and phenotype [48]. In normal condition, stroma components regulate tissue homeostasis and extra cellular matrix (ECM) integrity while, in pathologic status, they release cytokines, chemokines and growth factors to modify the TME features [49]. A supportive milieu for the development of cancer and the spread of metastatic disease is produced by the cell-matrix interaction, which controls pathways involved in cell proliferation, differentiation, and migration [50,51]. The ECM represents also a reservoir of growth factors released upon tissue request [52]. For instance, the control of immune cell functions, neo-angiogenesis, and the modification of the tissue scaffold structure are all aspects related to the action of the transforming growth factor-beta (TGF-β) [53-56]. In addition, cancer cells overexpress a number of substances able to alter the ECM structure. LOX family oxidases and matrix metalloproteinases (MMPs) are two categories of enzymes implicated in the alteration of the TME mechanical properties [48]. By several crosslinking and collagen stabilization, the LOX family controls structural integrity and tension strength. The hypoxic microenvironment that characterizes the cancer niche promotes LOX overexpression, supporting ECM rigidity and tissue stiffness [57]. These alterations have been demonstrated to increase cancer cell growth and migration to the surrounding tissues.

Fibroblasts, one of the main stroma components are crucial to the growth, motility, angiogenesis, and metastatic spread of tumors [58]. Through the transition to cancer-associated fibroblasts (CAFs), they may acquire a malignant phenotype. In fact, CAFs support the cancer progression through the paracrine release of pro-cancer factors (such as HGF, TGF, VEGF, and NK4), the deposition and remodeling of the ECM, and immunological modulation [59]. Like tumor cells, CAFs secrete MMPs. As already reported, MMPs play a role in the mechanical modification of tissue scaffolds in addition to several other processes including immunological control, angiogenesis, intravasation, induction of the pre-metastatic niche, and inflammatory control [60–62]. CAFs are able to modulate both innate and adaptive immunity. These alterations are driven by the secretion of molecules implicated in the recruitment of specific cell populations (e.g. monocytes and neutrophils) and induction of their immunosuppressive phenotypes [62]. Additionally, malignant cells induce

NF- pathway activation, resulting in pro-inflammatory signaling. As a result, immune cell control becomes dysfunctional, resulting in abnormal B cell development and CD4 T-cell differentiation [62]. In accordance to the cancer site location, CAFs have been found to have heterogeneous origins [62]. CAF development can occur in different cell types. Normal fibroblasts and mesenchymal stem cells (MSCs) are the primary sources of CAFs, although other cells can also develop into activated fibroblasts, including stellate cells, fibrocytes, endothelial and epithelial cells [64,65].

The cancer stem cell (CSC) theory, developed more than ten years ago, asserts that the tumor has its own stem cell clones with the ability to self-renew, and links the development of these malignant cells to changes in regulatory pathways caused by genetic mutations in the population of healthy stem cells [66]. The preservation of CSC stemness depends on the tumor niche's microenvironment. In this setting, CAFs stimulate pathways such the NOTCH and WNT signaling cascades that are related to the stimulation of stemness processes. While WNT supports the development of CSCs from both normal stem cells and non-stem cancer cells, the NOTCH pathway contributes to the suppression of cell differentiation [67]. Hypoxia also stimulates the cancer cells dedifferentiation in CSCs [68] and oxygen reduction necessary for epithelial mesenchymal transition (EMT), a process involved in metastatic development. In non-stem cancer cells, EMT controls cancer cell plasticity by promoting CSC phenotypic differentiation and self-renewing ability [68]. Many studies demonstrated that CSCs play a part in chemotherapy resistance, both in hematologic and solid cancers [69]. The low drug sensitivity is ascribed to increased drug efflux-related transmembrane protein transporters (ATP-binding cassette) production, increased expression of EMT-associated genes, and antiapoptotic proteins [69,70].

Many other cell populations, including MSCs, adipocytes, endothelial progenitor cells (EPCs), macrophages, and myeloid-derived suppressor cells (MDSCs), are implicated in the interaction between cancer and healthy components [71]. In conclusion, normal tissue components significantly contribute to tumor processes, and this fact must be taken into account to conduct both in vitro and in vivo studies.

1.5 Immune system influence in HNSCC

Inflammation promotes the development of cancers, including HNSCCs [72]. Different studies indicate that various immune cell populations infiltrate the tumor niche and secrete several cytokines, growth factors, and proteolytic enzymes (such as TGFβ, matrix metallopeptidases (MMP) and VEGF) which might affect cell metabolism and the TME phenotype [73]. Although, inflammation may support the decrease of neoplastic growth, an immune response that is controlled by cancer cells provides a chance for the growth of malignant cells that can resist to the immune system's damaging effects. In HNSCCs, it has recently been reported the impaired activity of systemic and local inflammatory responses [72]. Indeed, cancer cells can alter the

polarization of different immune cells populations. Several immune cell populations of both innate and adaptive immune responses infiltrate the HNSCC TME: tumor associated neutrophils (TANs), dendritic cells (DCs), mast cells, tumor associated macrophages (TAMs), natural killer (NK) cells, myeloid-derived suppressor cells (MDSCs), B cells, and T cells. All these cells influence the HNSCC onset and progression. Tumor infiltration of immune suppressor cells, macrophages M1, TAN N1, NK, CD8+ T cells and T helper 1 and 17, are normally associated with a favorable outcome [74,75]. On the other hand, immunosuppressive cells, such as macrophages M2, TAMs, T helper 2, MDSCs and TANs N2, are correlated with a bad prognosis.

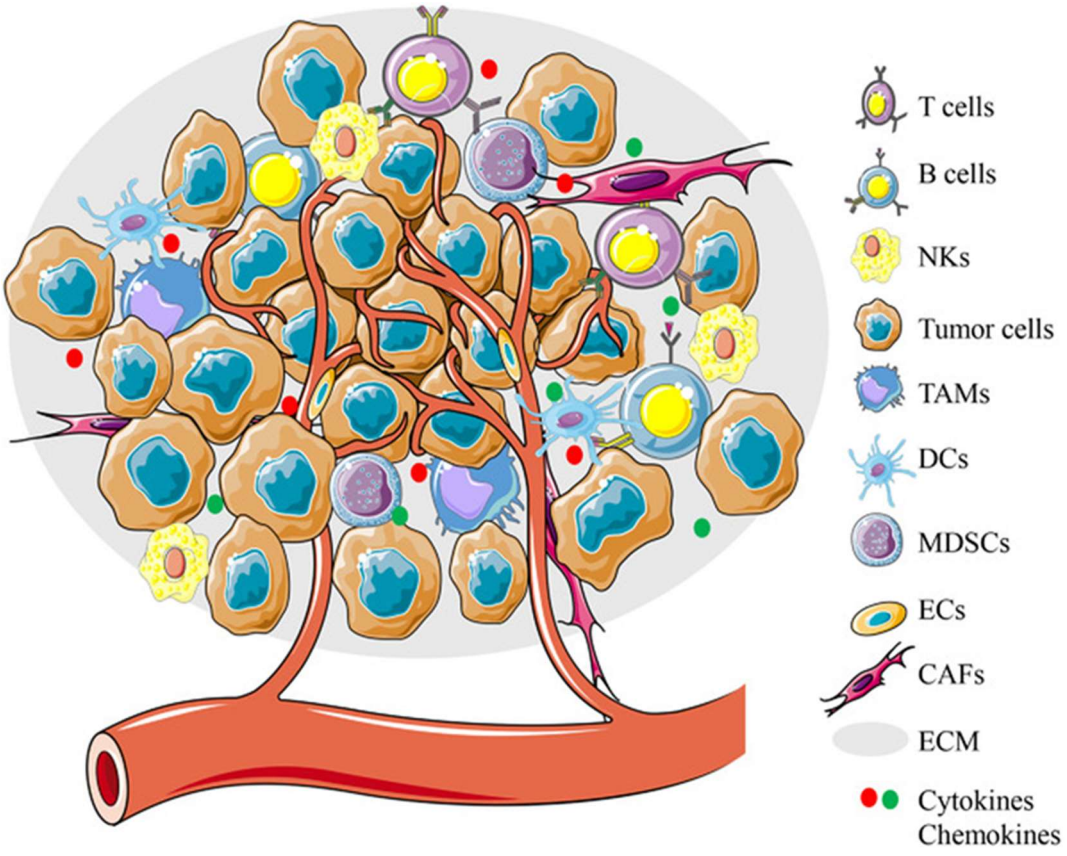

Figure 2: Components of the TME [72]

T lymphocytes represent one of the first actors of immune system. These cells are divided in two main groups: CD4+ and CD8+ T lymphocytes. CD4+ T lymphocytes can be divided into two further subgroups characterized by distinct features: regulatory T (Treg) and helper T (Th) cells. On the other hand, cytotoxic CD8+ lymphocytes carry out important antitumor activities. They recognize and fight tumor cells and for these reasons, their presence in the TME is associated with a good prognosis [76]. Th cells and Tregs display opposite functions. Th cells support the CD8+ T lymphocytes antitumor effects while Tregs inhibit the functions of CD8+ T cells promoting immunosuppressive effects. In HNSCC patients, an increased amount of

circulating Tregs is associated to unfavorable outcomes while, cytotoxic CD8+ lymphocytes infiltration represents a good prognostic factor [77].

Unfavorable patient outcomes were associated to the presence of elevated levels of tumor-infiltrated or circulating neutrophils [78]. TANs are a further population of cancer infiltrating immune cells observed in solid tumors, including HNSCC [79]. Their roles include the stimulation of cancer cell proliferation and metastasis, angiogenesis processes and TME matrix degradation [80]. On the other hand, TANs also perform antitumor actions, such as the induction of malignant cell apoptosis and triggering CD8+ T lymphocyte proliferation [80].

MDSCs represent a kind of immature immunosuppressive cells that are divided in two main groups: monocytic and granulocytic. Their recruitment in the TME is stimulated via chemotaxis by, granulocyte macrophage-colony-stimulating factor (GM-CSF), VEGF, IL-1β, IL-6 and IL-10 [81]. MDSCs conduct several biochemical processes and interactions with other cell populations (such as TAMs and DCs). For example, MDSCs are able to alter the NK cell activities, decreasing the NK cell-based immunotherapy efficacy in HNSCC [82].

Recently, several studies supported the key role of NK cells in initiating adaptive immunity [83]. This activity is driven by the expression of IFN-γ, a dimerized soluble cytokine able to promote and activate the infiltration of Th1 cells and MDSCs [83]. NK cells contribute to both innate and adaptive immune responses. Their interaction with MHC class I on cancer cells surfaces induces cell recognition, and balancing between inhibitory and stimulatory signals. NK cells are considered an immunotherapy prime target due to their influence on adaptive immunity and to their cytotoxicity toward cancer components. HNSCC patients display a high degree of NK cells infiltration that is associated to favorable prognosis [84]. As a result, the activity of NK checkpoint receptors has been studied and gained significant interest in cancer immunotherapy [84,85].

1.6 The role of Monocytes in the TME

Monocytes represent one of the major circulating cellular fractions of innate immune cell population. They are responsible of many physiological processes: i) activation of the immune response, ii) maintenance of the tissue homeostasis, iii) driving the response to pathogen infections [86]. Currently, different studies have described monocytes as important regulators of cancer processes. Depending on the subset, these cells can display opposite roles in promoting cancer progression or preventing the metastasis development [87,88]. In this scenario, monocytes represent the main source of DC and TAM infiltrating the TME [89]. In order to understand the processes used by cancer cells to evade the immune system and increase the effect of immunotherapies, it is important to explore and characterize the monocytes heterogeneity and their role in all the stages of cancer growth and progression.

In the last decades, the view of monocytes as a homogenous cell population has changed and now these cells are described as a heterogeneous group with distinct functions in response to specific stimulations. MHC class II (MHCII), Human Leukocyte Antigen – DR isotype (HLA-DR), CD86 and CD11b integrin are markers universally expressed by human monocytes. Human monocytes are divided in 3 subsets depending by the expression of CD14 and CD16: classical monocytes ($CD14^+/CD16^-$), non-classical monocytes ($CD14^{low}/CD16^+$) and intermediate monocytes ($CD14^+/CD16^+$) [90]. These groups represent the classical subdivision but recently transcriptional profiling analysis well described the main features of monocytes sub-populations and allowed the identification of two novel subsets [91]. Thus, the $CD14^+/CD16^+$ intermediate monocytes are divided in classical (Mono1) and non-classical (Mono2) clusters and the remaining monocytes form two new clusters, named Mono3 and Mono4 that represents the 12% of the total monocyte population. Respectively, the Mono3 subgroup expresses high levels of markers associated to differentiation, proliferation and trafficking while the last subset displays NK and T cell cytotoxic gene signature activation. Further studies are needed to explore and deeply characterize the functions of these novel subsets [91].

Despite similar phenotypes, monocytes can sustain or fight the cancer development based on the features of TMEs, tumor site and type, tumor stage and experimental model. Tumor niches release molecular signals to recruit monocytes both in the early tumor stages and in the development of distant metastasis [92,93]. Different studies have demonstrated the role of CCL2 in monocyte recruitment. Indeed, the expression of CCL2 increases during the tumor progression phases [94]. The trafficking of monocytes between organs (such as spleen, bone marrow and blood) during the development of cancer lesion should be extensively studied.

Phagocytosis and cytokine-mediated cell death are the two principal strategies used by monocytes to directly kill cancer cells. For example, IFN-γ or IFN-α induce the expression of the TRAIL protein in peripheral blood monocytes, which has the function to activate cell death pathway in malignant cells [95]. Differently, both $CD14^+$ and $CD16^+$ monocytes subsets can induce apoptosis through Antibody (Ab)-dependent cellular cytotoxicity [96]. Physical contact and TNF-α signaling represent two factors required by $CD16^+$ monocytes for the activation of cytolytic process [96]. On the other hand, tumor cells can alter the monocytes phenotype in order to support their growth.

Phagocytosis represents the main immune response mechanism mediated by monocytes to kill cancer cells [97]. In the blood circulation, cancer cells evade the phagocytosis through the expression of CD47, an integrin associated protein implicated in a range of cellular processes, including migration, proliferation, adhesion and apoptosis [98]. SIRPα, the CD47 ligand, is highly expressed by circulating monocytes but CD47/SIRPα signaling is poorly explored in tumor development although it is implicated in monocyte-mediated regulation of metastasis. Non-classical monocytes represent a suitable immune cell population for the elimination of cancer cells and debris due to their patrolling action and long lifespan. This monocyte subset migrates within

tumor tissues, to engulf malignant material and to release cytokines involved in the antitumor immunity regulation [88,99].

As other components of the TME, also the features of ECM are dysregulated during oncogenesis, such as biomechanical stimuli, cell migration and molecular pathways [100]. Classical monocytes take part in ECM remodeling processes. These cells promote the fibrin cross-linking, accumulated by leaky vasculature, through the expression of factor XIIIA [101]. In non-small lung cancer, the increased stiffness connected with the monocytes action supports the metastatic cancer cell invasion and disease progression [102]. Other players of the ECM degradation are the TAMs derived from $CCR2^{+}$ monocytes by the endocytosis of deposited collagen [102]. Further studies are needed to investigate the crosstalk between ECM and monocytes to understand ECM contribution to the 3D matrix organization, and the regulation of monocyte fate in cancer tissues.

1.7 Macrophages role in HNSCC

The immune cell populations, including macrophages subgroups, constitute one of the major components of TME and represent a link between the innate and adaptative responses. Macrophages are divided in two phenotypic groups: M1, considered as proinflammatory and antitumoral; and M2, possessing immunosuppressive and pro-tumoral activities [103,104]. M1 macrophages polarization is induced by the action of interferon-γ lipopolysaccharides (LPS) and tumor necrosis factor α (TNFα). The antitumoral effect of M1 macrophages is due to the secretion of high level of human leukocyte antigen (HLA)-DR, CXC ligand 10 (CXCL10), interleukin (IL)- 1β, IL-6 and TNFα [105]. Differently, the activation of molecular pathways, such as CD47/SIRPα, IL6, CSF-1, CCL-2 and PD-1/PD-L1 axis, leads to M2 macrophages phenotype. This cell subpopulation is responsible of the directly or indirectly increase of local inflammation through the expression of TGFβ, VEGFs, MMPs, CC ligands, IL-4 and IL-10 [105]. The development of an inflammatory microenvironment increases the aggressivity of the malignant cells responsible of tumor progression, metastasis and drug resistance.

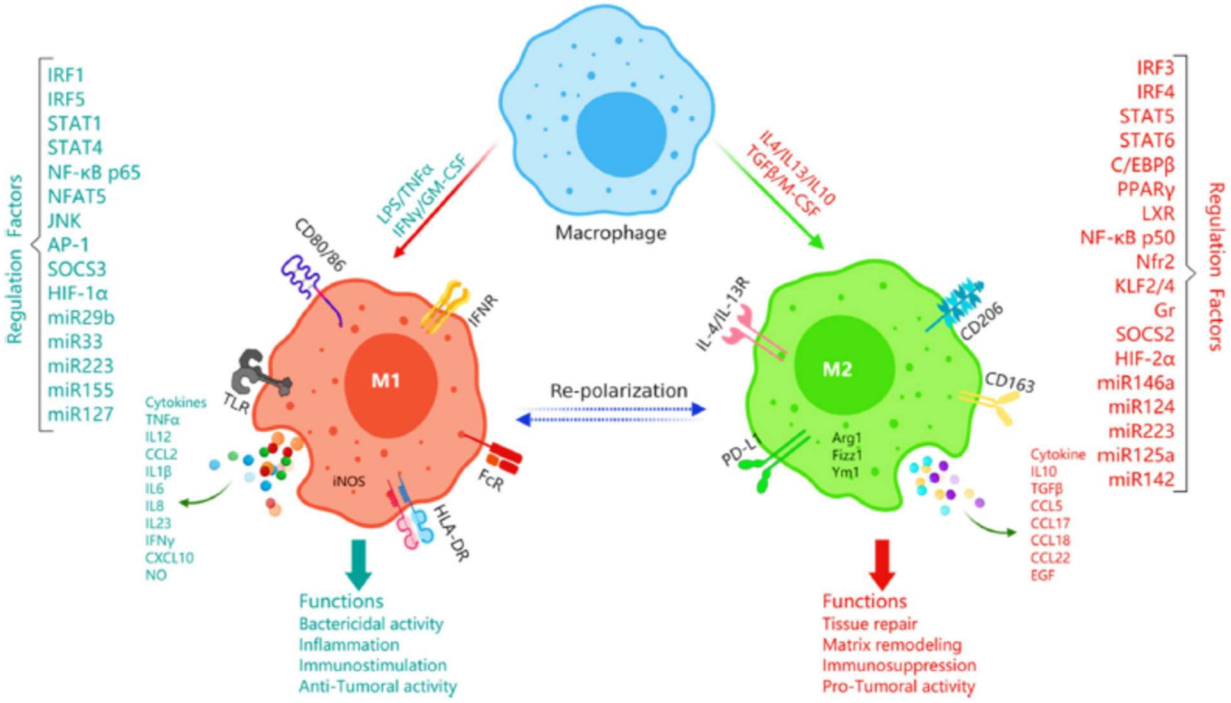

Figure 3: Schematic summary of macrophages polarization markers, regulation factors and functions. [Li C. *J Immunother Cancer. 2021*]

Cancer cells can activate the tumor-promoting functions of macrophages due to the secretion of growth factors, proangiogenic signals and suppressive T-cell effectors [106,107]. In particular, the malignant components polarize macrophages in TAM, located inside or in proximity of the TME. The main function of TAMs is related to the pro-tumoral activity of the M2 macrophages [108]. Indeed, in many solid tumors the infiltration of TAMs is correlated with poor outcomes [109]. In HNSCCs, this observation was reported in Oral Squamous Cell Carcinoma (OSCC) but is less clear in the other HNC subgroups [110].

The main method to identify TAMs is immunochemistry. CD68 and CD163 represent the most frequently used markers to identify and isolate TAMs from the other cell populations [111]. CD68 is a pan-macrophage marker that allow identifying macrophages regardless the phenotype, but it is also expressed by others hematopoietic cells such as: neutrophils, monocytes, dendritic cells, mast cells and basophils [112]. Instead, CD163 is a marker used to discriminate between M1 and M2 phenotypes as it is expressed only by M2 macrophages [111].

The TAMs distribution inside the tumor tissue area has not been deeply studied in HNSCCs. This biological aspect is particularly important because studies reported co-localization with PD-L1 expression and modulation of immunotherapy response. In HNSCCs, it is reported the presence of PD-L1-positive TAM in the edge of tumor tissues and the surrounding inflammatory stroma [113]. In this context, these cells could contribute to adaptive resistance of PD-L1 positive HNSCCs due to a PD-L1 immuno-protective “barrier”

around the cancer tissue [113]. This TAM distribution could be associated to PD-1 inhibitors resistance and to some clinical features, such as tumor stage or HPV positivity.

The development of next generation sequencing (NGS) technologies has allowed the characterization of the different macrophages populations by a genetic point of view [114]. Genome-wide studies identified pattern of genes differentially expressed between macrophages isolated from healthy and neoplastic tissues [115]. The main differences concerned pathways involved in immune and angiogenic processes and highlighted that WNT signaling is highly activated in pro-invasive TAMs, promoting EGF-CSF1 paracrine loop involved in metastasis development [116]. Moreover, single-cell sequencing analysis have simplified the profiling of TAM populations across the different kinds of cancer. Some phenotypic characteristics were conserved between tumors, including a fraction of pro-angiogenic TAMs expressing high levels of Secreted Phosphoprotein 1 (SPP1), a protein associated to poor prognosis [117]. On the other hands, these analyses identified different TAM subsets among cancer types, confirming the heterogeneity of these immune cell populations in tumors. For example, Triggering Receptor Expressed On Myeloid Cells 2 (TREM2) positive TAMs accumulated in injured livers including hepatocellular carcinoma tissues (HCC) [118]. The inhibition of TREM2 expression increased tumor growth in mice affected by HCC, suggesting two distinct roles of the protein, one protective and one pathogenic [119].

TAMs could be used as target for innovative therapies, but further investigations are needed. One approach currently studied in different clinical trials is the use of colony stimulating factor 1 receptor (CSF-1R) inhibitors [121]. These anticancer agents may also be tested in HNSCCs, especially primary sites and OSCCs. Another approach could be treating patients with compounds able to reprogram TAMs phenotype from M2 to M1 polarization. The re-polarization process could stimulate the immune response in order to increase the response to immune checkpoint inhibitors [118]. For example, the inhibition of the pro-tumor capability of TAM can be induced by treatments with CD40 agonists, a marker expressed by some TAM sub-populations [120]. The main effect was the production of IL-12 and thereby CD8+ activation. Several clinical trials tested the efficacy of CD40 agonists and reported moderate effects and some toxicity [120]. As in other solid tumors, drugs combinations focused on the synergy between different compounds represent a research topic for future innovative therapies.

1.8 3D models in the field of oncology

Cancers are dynamic tissues composed of malignant and normal cell populations in continuous co-evolution and supported by extracellular 3D structures. Continuous remodeling of the ECM is a typical feature of the cancer cells [122]. Its complexity and its crosstalk with other TME components makes it impossible to

reproduce ECM by common monolayer supports [123]. To overcome these limitations, several 3D models have been generated to reproduce more realistically the tissue architecture.

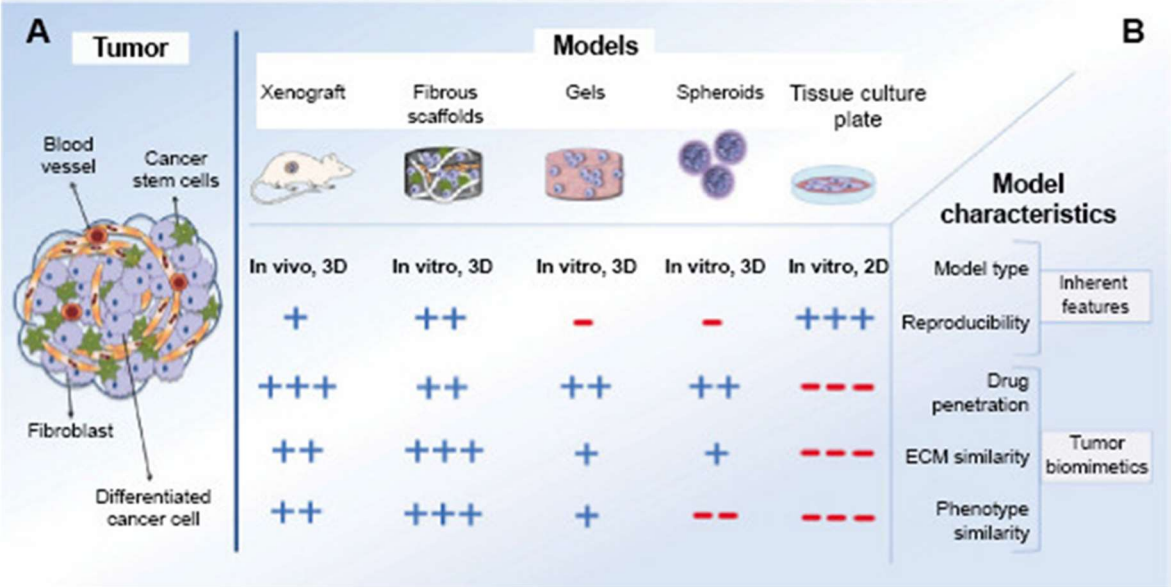

Figure 4: Schematic picture of preclinical models' features [Khadidiatou G. *Breast Cancer*. 2016].

Scaffold-free and scaffold-based *in vitro* cultures are two different approaches to mimic the TME. Regarding scaffold models, synthetic or biologically derived matrix materials have been used to develop innovative culture systems, and engineered gels are one of the most used technologies. In the last decades, several methods have been validated to synthesize polymeric hydrogels. One example is the use of end-functionalized multi-arm polyethylene glycol (PEG) macromers to synthesize hydrophilic and inert models through the chemical crosslinking of functionalized polymers [124]. Zhang M. et al. used a synthetic polyester-based scaffold system to study the radiotherapy effects on HPV positive and negative OSCC cell lines [125]. The results show how the device reproduces the same radio-sensitivity observed in OSCC patients, with a higher effect detected on HPV positive cells than the negative counterparts [124]. Biomimetic porous devices represent one of the most used technologies in the field of tissue engineering applications. The components for the generation of the scaffold models can be selected from materials of different origin: synthetic polymers (such as poly(l-lactic-co-glycolic acid) PLGA, polyurethane (PU) or poly(d,l-lactide) (PDLLA)), non-polymeric materials (i.e. fibronectin, collagen, or Matrigel) and biological-derived substances such as decellularized matrices [126]. The most efficient materials to reproduce faithfully the natural pathophysiological tumor features is represented by biologically derived components [123]. Collagen is the most abundant component of human connective tissues; thus, collagen-based scaffolds are widely employed as ECM mimetic devices [127]. Recent studies have demonstrated that these devices are able to activate different drug resistance mechanisms and induce pathological features typical of the cancer cells seeded

[128,129]. Miserocchi G. et al. report how this device mimics better than the common monolayer culture different biological features of OSCCs depending on the HPV status [130]. These results support the employment of collagen-based scaffolds for the development of drug screening platforms in the field of precision medicine to select the most effective therapy for each patient.

In the 80s, scaffold-free 3D models started to be generated and they are still used in cancer research [131]. These spherical cancer models have different nomenclature depending by the sample origins. In this manuscript, we use the term “spheroid” to identify all the spherical cancer systems. The spherical structures are generated by the aggregation of single or small cluster of cells driven by cell–cell interactions. These models display superficial and inner areas with different nutrients and oxygen gradients due to their spherical shape, mimicking the structural feature of cancer masses [132]. The spheroids development consists in an initial exponential cell growth, slowly replaced by a stable proliferation phase characterized by an increased number of quiescent cells [133]. These aspects make scaffold-free cultures excellent models to mimic the spatial distribution of cancer cell sub-clones. Moreover, the cancer cell sensitivity to radiation and anticancer agents is affected by permeability and oxygen tension, making spheroids excellent systems for in vitro drug screening studies [134-136]. Spherical culture can be obtained starting also from patient-derived samples. These 3D cultures, named organoids, are self-organized structures originated from sub-clones with stem properties and can be easily used for drug screening assays [137]. Lim Y.C. et al. developed for the first time squamo-spheres, organoids obtained from HNSCC human tissues cultured in serum-free media [138]. In 2019, Driehuis E et al. tested the efficacy of standard and innovative therapies on a panel of healthy and 31 malignant organoids of HNSCCs [139]. The drug-screening platform included not only anticancer compounds (targeted therapies and chemotherapeutic agents) but also combinations of the above-mentioned drugs and radiation exposure. Future clinical trials are needed to confirm the organoids ability to predict patients’ response to different treatments. In this context, ONCODE-P2018-0003 represents the only validation study in which organoids drug sensibility will be compared to the patients’ outcomes [140].

Up to now, we have reported 3D models generated from single cell suspensions obtained after tissue digestion. This approach favors the loss of both the matrix 3D structure and part of the cells belonging to TMEs [141]. The spatial interactions and the crosstalk between different cell populations that compose the tumor niches are key aspects to study cancer progression. To overcome these limitations, different approaches have been developed that do not need tissue digestion. One option is represented by patient-derived explants (PDE), used since the early 1950s [142]. The cultures are established by tissue fragments maintaining the endothelial, immune and stromal components as well as the ECM architecture of the original cancer [141]. In 1991, Vescio R.A. et al used a Histoculture Drug Response Assay (HDRA) to predict the treatment efficacy on patients affected by stomach and colorectal cancers and they showed a correlation rate of 92,1 % [143]. In the field of HNCs, CANScript is an *ex vivo* drug screening platform based on slices of

tissue samples seeded on coated supports or transplanted in animals as patient derived xenografts (PDXs) [144]. The two approaches showed a strong data correlation. Moreover, the platform stratified the patients, treated with combination of cisplatin, 5-fluorouracil and docetaxel, in partial or complete responders and non-responders [144]. Despite the excellent preclinical results, these platforms are not applied yet in clinical practice.

2. Project aims

The interaction of cancer cells with the tissue microenvironment and their crosstalk with healthy components are two important features that influence the pathophysiological features of tumor diseases, included head and neck cancers (HNCs). Moreover, the improvement of systemic therapy and immunotherapeutic drugs, increases the need to better understand the biological mechanisms that drive the response of these innovative drugs. The interaction between different cell populations, and in particular of the immune system components, represents a complex aspect to study through the common monolayer cultures. The project aim is the study of the crosstalk between HNC cells and CD14+ monocytes in three-dimensional microenvironments. 3D collagen-based scaffolds represent one of the main models used to mimic the tumor niche. The cell types selected for the study are two immune cell populations (monocytes CD14+ and macrophages) and oral cavity squamous cell carcinoma (OCSCC) cell lines.

3. Materials and Methods

3.1 Collagen-based scaffold synthesis

Collagen devices were synthesized using chemicals produced by Sigma-Aldrich (St. Louis, USA). Bovine collagen type I was suspended and precipitated to pH 5.5. The collagen was crosslinked with 1% 1.4-butanediol diglycidyl ether (BDDGE) to stabilize the collagen structure and control its porosity. The final monolithic scaffold was generated using a freeze-drying process. Obtained scaffolds were washed in 70% ethanol for 30' for sterilization and followed by two washes of 20' in sterile phosphate buffered saline (PBS).

3.2 2D and 3D Cell Cultures and Reagents

UPCI:SCC154 OCSCC cell line and UM-SCC6 HPV negative OSCC cell line were purchased from American Type Culture Collection (Rockville, MD, USA) and MD Millipore (Merck S.p.a., Darmstadt, Germany) respectively. UPCI:SCC154 cells were maintained in Eagle's Minimum Essential Medium (ATCC, Rockville, MD, USA) supplemented with 1% of penicillin/streptomycin (PAA) and 10% of heat inactivated fetal bovine serum (FBS, Euroclone, Milan, Italy). UM-SCC6 cell line was maintained in DMEM High Medium (Euroclone) supplemented with 1% of PAA, 1% L-Glutamine (PAA, Piscataway, NJ, USA), 1% Non-Essential Amino Acids (Euroclone) and 10% fetal bovine serum. Cells were counted and seeded in 2D plastic supports or in 3D collagen-based scaffolds. Both cell lines were maintained in a 5% CO2 atmosphere at 37°C.

3.3 CD14+ monocytes isolation

Human CD14+ monocytes were isolated from the PBMC of healthy donors, who gave written informed consent to take part in the study. PBMC were isolated from buffy coats by Ficoll density gradient. Briefly, EDTA whole blood (50 mL) was diluted 1:1 with PBS, layered on lymphocyte separation media (Lymphosep, Biowest, Nuaillé, France) and centrifuged without brakes at 1000×g for 20 min. The PBMC layer was collected and washed twice with PBS and treated for 2 min on ice with ACK lysis buffer. After having washed them twice with PBS, cells were counted and sorted using antihuman CD14 MicroBeads (Miltenyi Biotec, Bergisch Gladbach, Germany). Cells were resuspended in 80 µl of buffer every 10^7 cells and added 10 µL of CD14 MicroBeads per 10^7 total cells. The suspension was mixed and incubated for 15' in dark at 4°C. Cells were washed by adding 1−2 mL of buffer and centrifuged at 300×g for 10 minutes. A Column for cell sorting was placed in the magnetic field of a suitable MACS Separator and prepared by rinsing with the appropriate amount of buffer (according to the manufacturer's instructions). The cell suspension was applied onto the column and washed three times by adding buffer. The cells were eluted and suspended in X-VIVOTM 15

Serum-free Hematopoietic Cell Medium (LONZA, Basel, Switzerland) supplemented with 2% of FBS and 1% of PPA.

3.4 Viability assays

Cells viability was measured through MTT tests (Sigma-Aldrich) and ReadyProbes TM Cell Viability Imaging Kit (Blue/Green) (Thermo Fisher Scientific). Eight images for each condition were analyzed using ImageJ software to count blue and green cells (live and dead respectively). The growth curves were generated by performing MTT assay at 1, 2, 5, 7 days. Images of stained samples were acquired by confocal microscope (Nikon Corporation, Tokyo, Japan) and analyzed with the NIS Elements software (Nikon Corporation, Tokyo, Japan). For each sample, 4 images were acquired in the edge area and 4 images in the inner area of the 3D devices.

3.5 Immunohistochemistry

Collagen-based scaffolds were embedded in paraffin, using cryomold (25 mmx20mmx5mm). 5-µm-thick slides were used for staining to evaluate the culture's morphological features and HIF-1α expression. The samples were hydrated and stained with hematoxylin and eosin (Sigma-Aldrich, Saint Louis, MO, USA) or with HIF-1α antibody (Ab). HIF-1α expression was determined in 5 µm sections with Ventana BenchMark ULTRA system (Ventana Medical Systems, Tucson, Arizona, USA) according to the manufacturer's instructions. Rabbit monoclonal anti-HIF-1α antibody (1:100, ab51608, Abcam, Cambridge, UK) was used to stain slice samples. Hematoxylin was used for counterstaining. Stained slides were analyzed by inverted microscope (Axioskop, Carl Zeiss, Gottïngen, Germany).

3.6 Cell cycle phases imaging in real-time

The fluorescence ubiquitination-based cell cycle indicator (FUCCI) was used to capture detailed cell cycle alterations. The transfection with lentiviral system to introduce FastFUCCI transgenes into our HNSCC cell lines was performed by an external member of the project in the MOGM (Microrganismi geneticamente modificati) facility of IRST. 2D and 3D cultures transfected with FastFUCCI plasmid were fixed with 4% Paraformaldehyde (PFA). The images were acquired using a Nikon Confocal Microscope.

3.7 Flow Cytometry

Polystyrene Round-Bottom Tubes (Corning Incorporated) were used for staining of the mono and cocultures subpopulations cell surface markers: CD14, CD45, CCR7, CD206, HLA-DR, PD-L1 labeled with APCVio770,

VioGreen, VioBlue, APC, PEVio770, PEVio615 fluorochromes, respectively, together with Live/Dead Yellow Fixable Stain (Thermo Fisher, Waltham, MA,USA). Each sample was incubated for 20' at RT protected from light. Then, the samples were washed and suspended in autoMACS Running Buffer (Miltenyi Biotec) to perform cytofluorimetric assay using the Attune™ Nxt Acoustic Focusing Flow Cytometer system (Thermo Fisher Scientific). The FCS data files were analyzed with FlowJo software (Inivai Technologies, Mentone, Australia).

3.8 Statistical analysis

Each experiment was repeated at least 3 times. Data are shown as mean ± standard deviation (SD), or mean ± standard error (SE), as stated, with n indicating the number of replicates. The two-tailed Student's t-test was used to define the differences between groups and p values < 0.05 were considered significant.

4. Results

4.1 Characterization of monocytes CD14+ 3D monoculture

Collagen-based scaffolds were obtained through pH-driven self-assembly method and a freeze-drying procedure. 48-well plates were used for the tubers' synthesis and, therefore, the devices diameter has a mean of 10.5 mm (Figure 1A). Collagen tubers were cut with a scalpel in slices of about 1.5 mm (Figure1B). Scanning Electron Microscopy (SEM) images showed reproducible morphology and pores structure, with mean size of 197 ± 25 µm (Figure 1C).

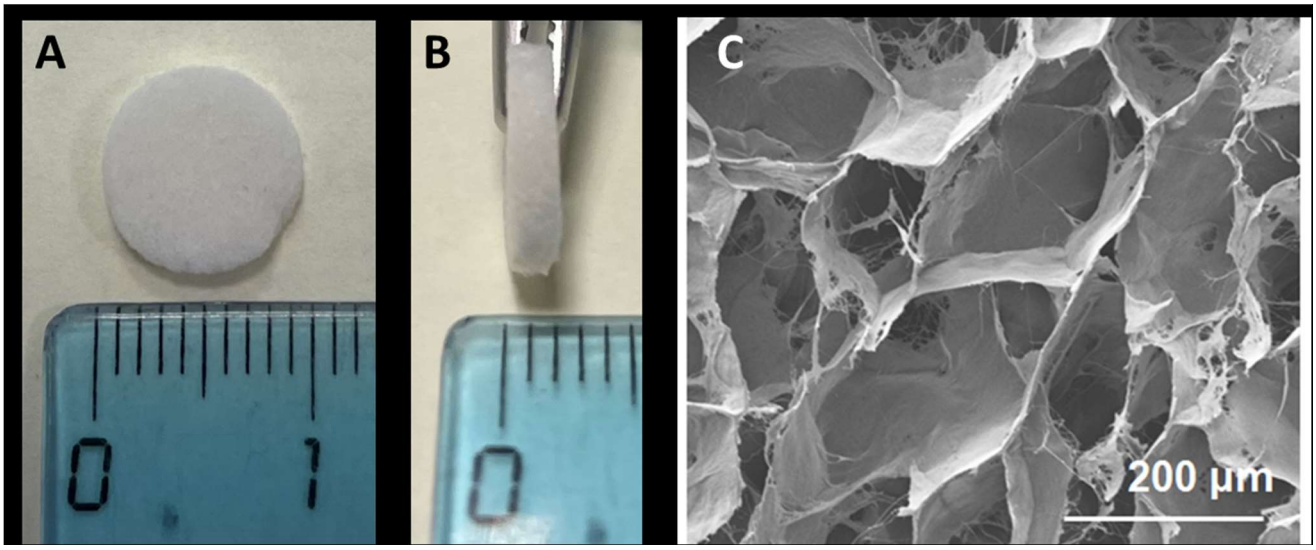

Figure 1: Collagen-based scaffold structure characterization; (A,B) photos of the upper and lateral sides of the device (C) SEM image of the scaffold structure showing porous structure of scaffold surface (scale bar: 200 µm).

In order to select the best parameters to develop the 3D monocyte culture, we have tested different cell concentrations and culture media. We checked two parameters: the percentage of cells not bound to the collagen fibers (floating cells), and cell viability.

We have tested three media formulations (RPMI + 10% FBS, Xvivo TM10 + 2% FBS and a mixture of 50% of Xvivo and 50% of tumor media) and two cell concentrations (1,75 x 10^6 and 2,5 x 10^6). The media conditions were selected based on the media used by other scientists for monocyte cultures maintenance. In order to study co-cultures with a ratio of 1:1 between monocytes and tumor cells, the monocytes' concentrations were selected based on the half of the total cell number seeded in two published articles that used collagen-based scaffolds [121,123].

The total number of cells not bound to the collagen structure showed a value between 12% and 17% (Figure 2). The differences in the percentages of floating cells in the different concentrations and media were not significant.

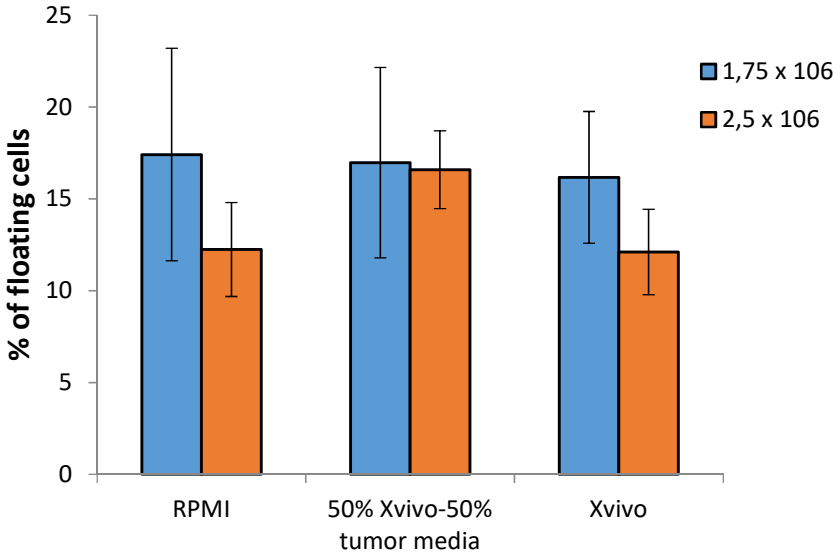

Figure 2: Percentage of floating cells in the culture media not bound to the collagen fibers at 48h post seeding. The percentage was calculated on the total number of cells seeded.

Then, we have compared the viability of the 3D cultures seeded in the selected media at selected concentrations. We have performed the experiments using the MTT assays at three different time points: 0h, 24h and 48h (Figure 3). The concentration of $1{,}75x10^6$ cells displayed higher viability compared to $2{,}5x10^6$ cell per scaffold in all the conditions. No significantly differences were identified between the media conditions with $1{,}75x10^6$ cells per scaffold. Differently, the concentration of $2{,}5x10^6$ cells showed media-dependent behaviors. The 1:1 Xvivo-tumor media induced higher viability and significantly differences with the other media. Based on this analysis, we have selected the mixed media 1:1 Xvivo and tumor media as the best monocytes co-culture condition.

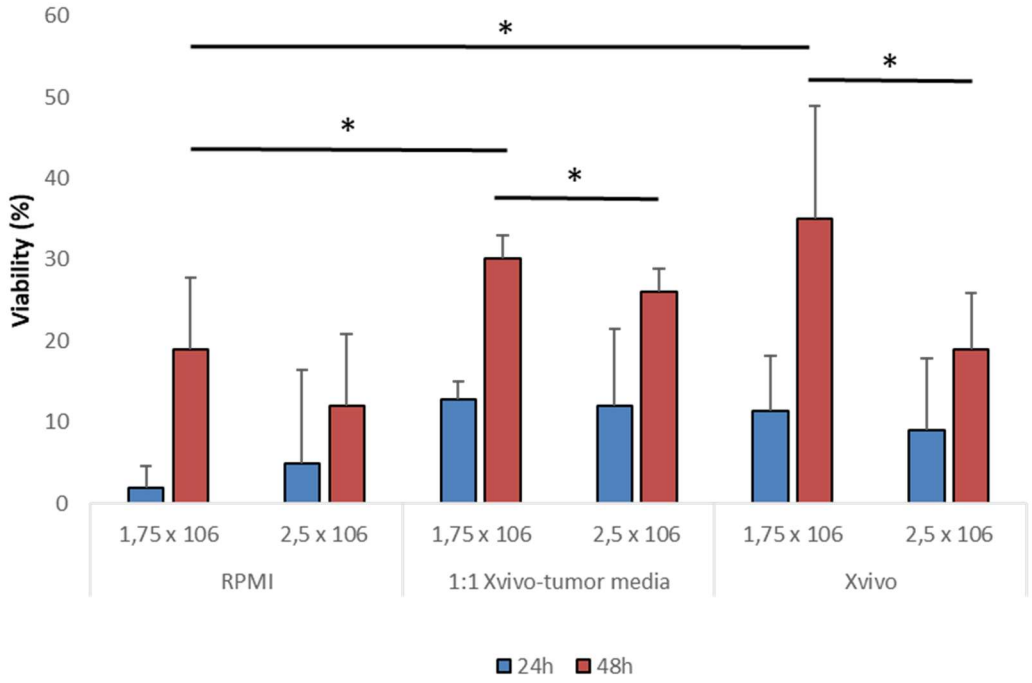

Figure 3: Viability percentage of monocytes at different concentration and culture medias. Data represent mean±S.D. (*) p <0.05, two-tailed Student's t-test.

Then, we have compared the viability of monocytes in 2D and 3D cultures using the MTT assays at different time points and concentrations in order to select the best co-culture parameters.

In plastic monolayer support, the cells viability increased slower than the 3D microenvironment. In particular, the concentration of 0,75 x 10^5 cells per well (96 well plate) tested in the 2D culture showed the highest cell growth ability (Figure 4).

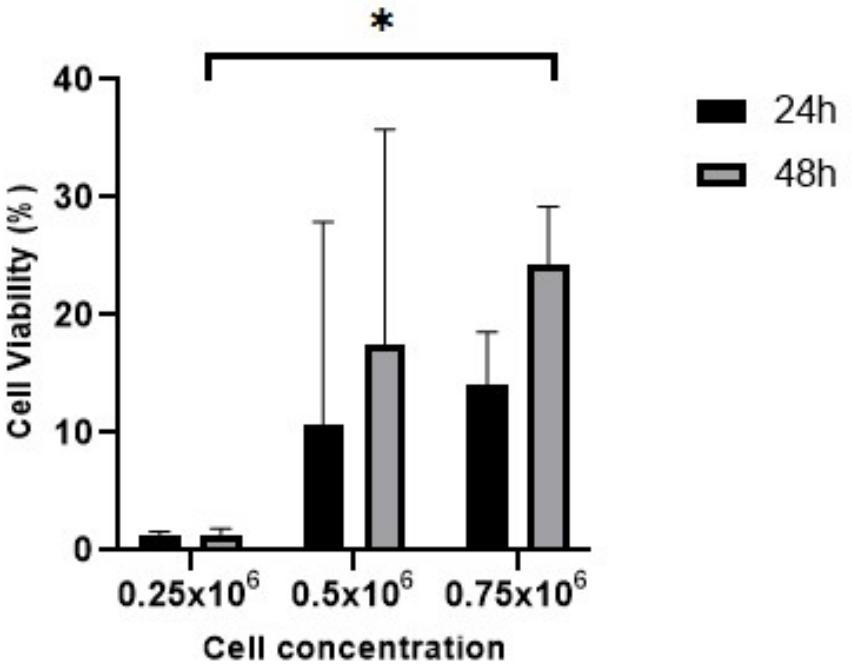

Figure 4: Cell viability percentage in 2D cultures. Data represent mean±S.D. (*) p <0.05, two-tailed Student's t-test.

In the 3D context, the concentration of 1,75 x 10^6 showed a higher viability at 48h compared to the condition with 2,5x10^6 monocytes per scaffold (Figure 5).

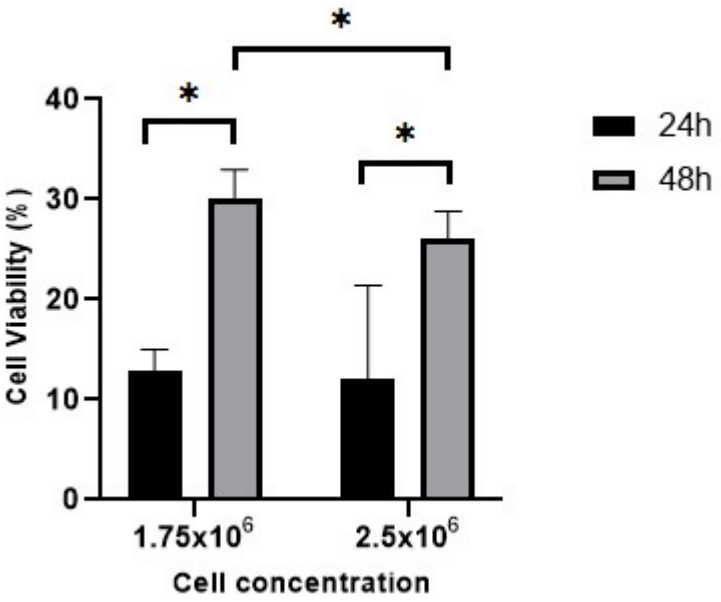

Figure 5: Cell viability in 3D cultures. The variations of viable cells percentage in 3D culture at 24h and 48h vs 2h post seeding.

We used ReadyProbes TM Cell Viability Imaging Kit (Blue/Green) (Thermo Fisher Scientific) to discriminate between live and dead monocytes inside the scaffold area. We have analyzed 8 images for each time point (0, 1, 2, 5, 10 days) counting the number of cells stained in blue and green (live and dead respectively). As expected, the results showed a progressive decrease of viable cells and an enhancement of dead monocytes over time (Figure 6 and 7).

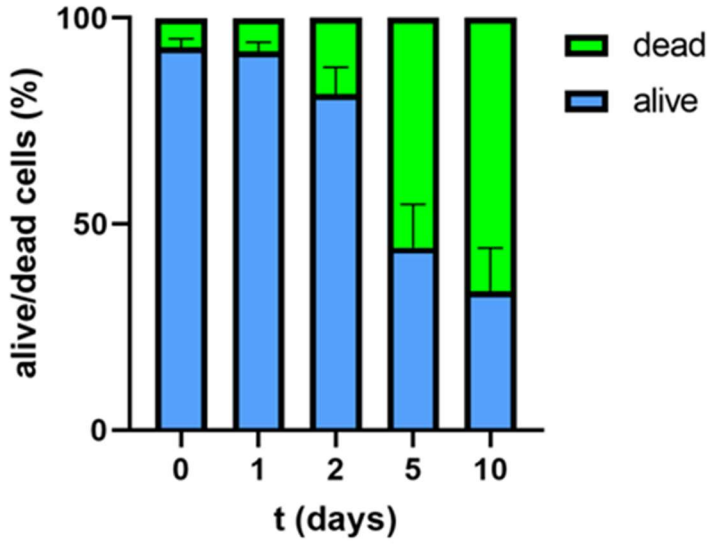

Figure 6: Percentage of live and dead monocytes seeded in 3D culture. The data were obtained in relation to the number of live cells (blue bars) and dead cells (green bars).

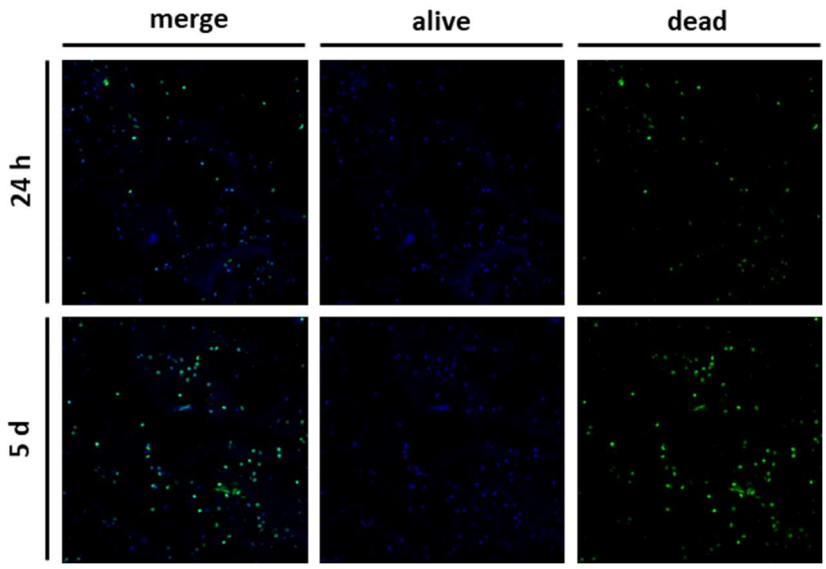

Figure 7: Representative images of live and dead cells in 3D culture at 24 h and 5 days post seeding (10X magnification).

In order to perform experiments with cells recovered from the 3D cultures, we have tested different protocols to digest the collagen-based scaffolds structure. We have measured the percentage of cells

recovered after 10' and 20' of dissociation treatment using different enzymes: Trypsin (Try), Collagenase (Col) or Tumor Dissociation Kit (TDK) (Figure 8). The 20' treatment with TDK showed the highest percentage of recovered cells, 81.1 %.

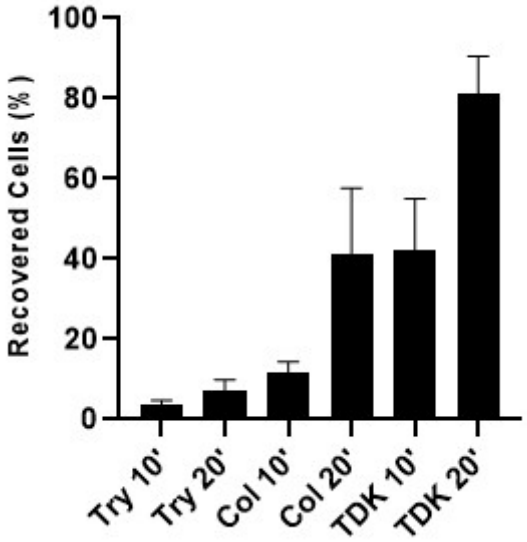

Figure 8: Percentage of monocytes recovered after digestion with: trypsin (Try), Collagenase (Col) and Tumor dissociation kit (TDK). The percentage was calculated on the total number of cells seeded.

We have quantified the number of live/dead cells after recovery using the cytofluorimetric technology. We stained cell samples with CD14 and CD45 to isolate the leukocyte population. After 48h, the monocytes displayed a viability of 98,2 % and 91.9 % in 2D and 3D cultures, respectively (Figure 9).

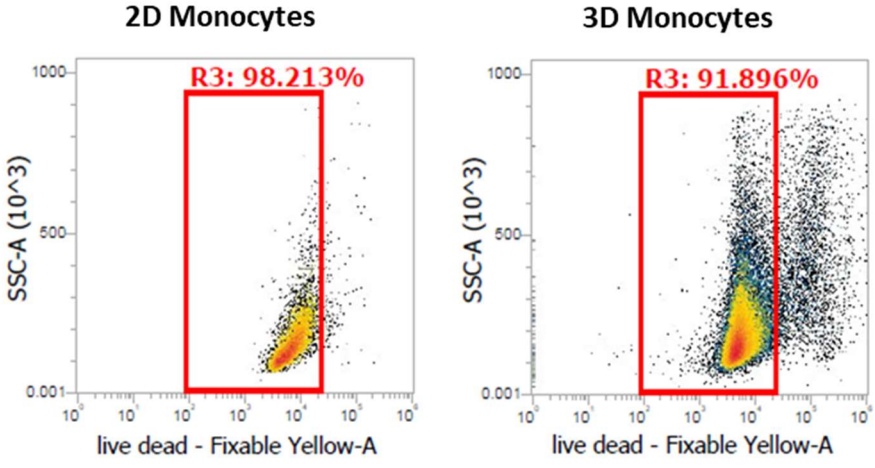

Figure 9: Representative dot plots of the percentage of live monocytes after recovery in 2D and 3D cultures at 48h post seeding.

At this point, we tested the expression of macrophages markers to understand the influence of the 3D structure on the monocyte polarization. In the 2D culture, the 40% of the cells expressed high level of CCR7 while almost the whole population is positive for HLA-DR (Figure 10).

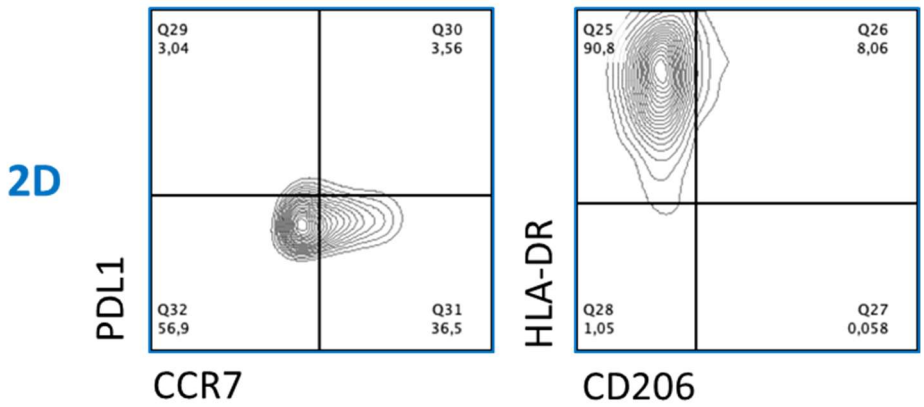

Figure 10: Representative M1 (CCR, HLA-DR) and M2 (PDL1, CD206) macrophages differentiation markers staining dot plots of 2D monocytes monoculture. The different area report the percentage of cells: negative for each markers (lower left), CCR7 or CD206 positive (lower right), PDL1 or HLA-DR positive (top left) and double positive (top right).

Conversely, the monocytes in the 3D scaffold showed lower level of $CCR7^{+}$ and $HLA\text{-}DR^{+}$ cells, respectively 19 % and 30.5 %, and a $HLA\text{-}DR^{-}/CD206^{+}$ population (18.4 %) and a double positive $HLA\text{-}DR^{+}/CD206^{+}$ group of cells (14.4 %) appeared (Figure 11).

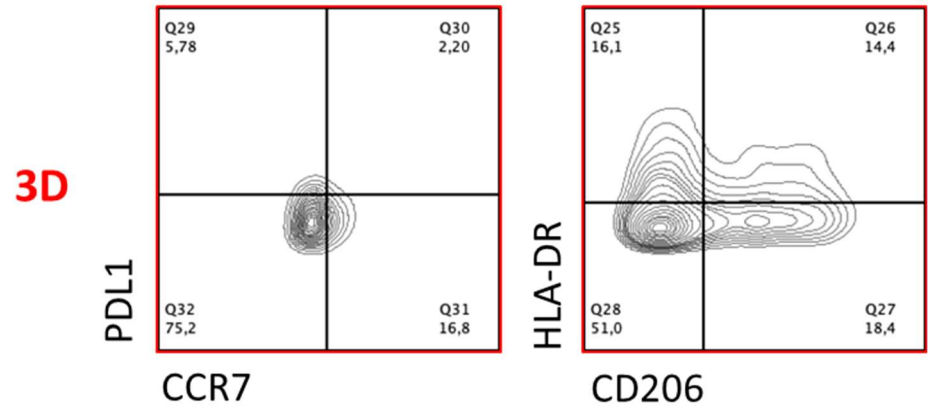

Figure 11: Representative M1 (CCR, HLA-DR) and M2 (PDL1, CD206) macrophages differentiation markers staining dot plots of 3D monocytes monoculture. The different area report the percentage of cells: negative for each markers (lower left), CCR7 or CD206 positive (lower right), PDL1 or HLA-DR positive (top left) and double positive (top right).

4.2 Characterization of HNSCC 3D monoculture

We have characterized the 3D cultures of HNSCC cell lines starting from the cell concentration selected for the monocyte 2D and 3D monocultures. We used the MTT assay to measure the proliferation rate at different time points (0, 1, 2, 5, 7 days). All the 2D HNSCC cultures displayed the classic exponential growth dynamic (Figure 12).

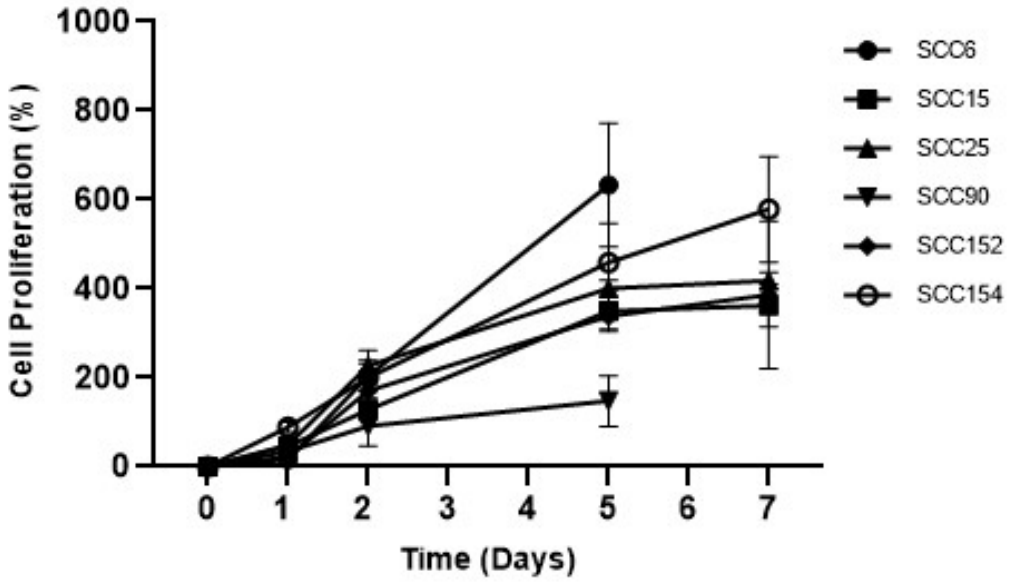

Figure 12: Fold changes in percentage of cell proliferation (relative to day 0) of HNSCC 2D cultures after: 1, 2, 5, 7 days.

On the other hand, the 3D cultures showed a constant decrease of cell viability. At 7 days post seeding, the fold changes in percentage of cell proliferation showed a value between -14.6 % of SCC6 to -45,6 % of SCC152 cells (Figure 13).

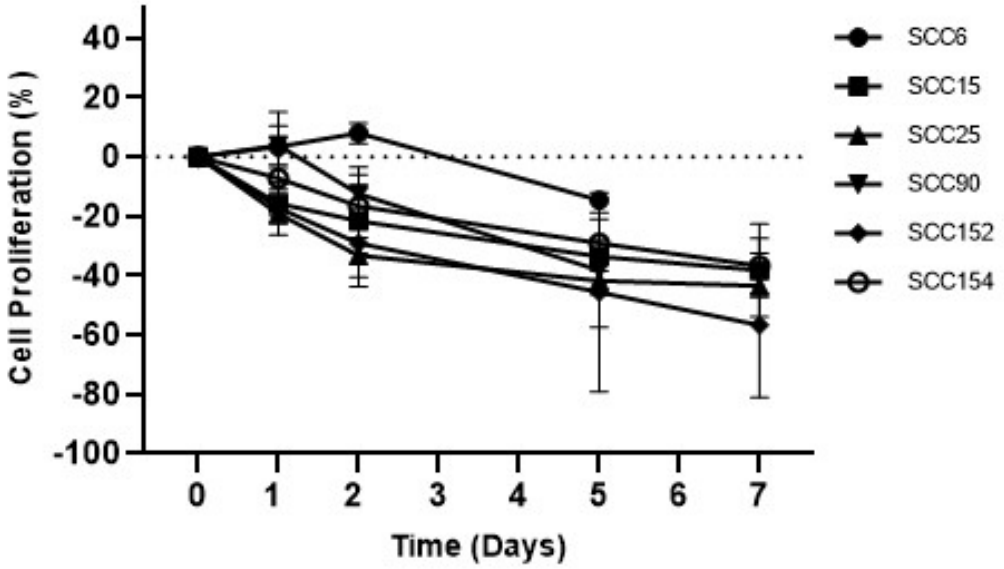

Figure 13: Fold changes in percentage of cell proliferation (relative to day 0) of HNSCC 3D cultures after: 1, 2, 5, 7 days.

We have tested the feasibility to cultivate primary cancer cells in the scaffold microenvironment. Two patient's tumor tissues of oral cavity SCCs, named HN2 and HN14, were processed as previously published [123]. We confirmed the presence of cancer cells in the scaffold area at 5 days post-seeding through the analysis of an experienced head and neck cancer pathologist and the expression of genes involved in cancer pathological processes. The two primary cultures showed different morphology characteristics. In the HN2 culture, we detected about 20% of cancer cells isolated or arranged in clusters and characterized by eosinophilic cytoplasm, central nucleolus and prominent nuclei (Figure 14 A and B).

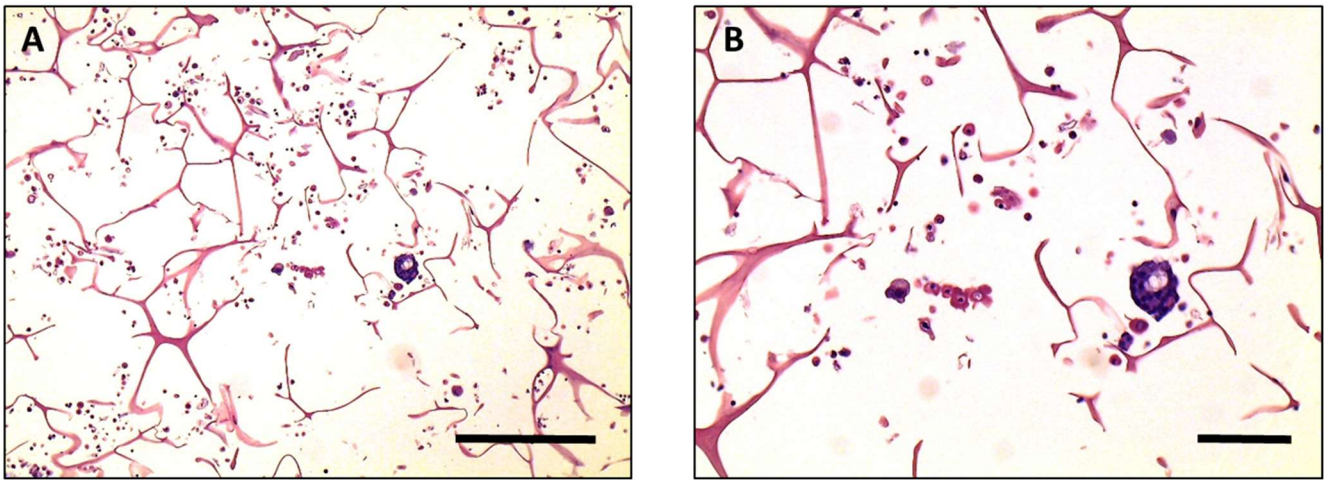

Figure 14: HN2 images of histological sections of the 3D primary culture at (A) 10X magnification (scale bars: 100 µm) and (B) 20X magnification (scale bars: 50 µm). The samples were stained with H&E.

On the other hands, the HN14 culture displayed about 30% of malignant cells with spindle morphology, large eosinophilic cytoplasm and nuclei with dispersed chromatin (Figure 15 A and B).

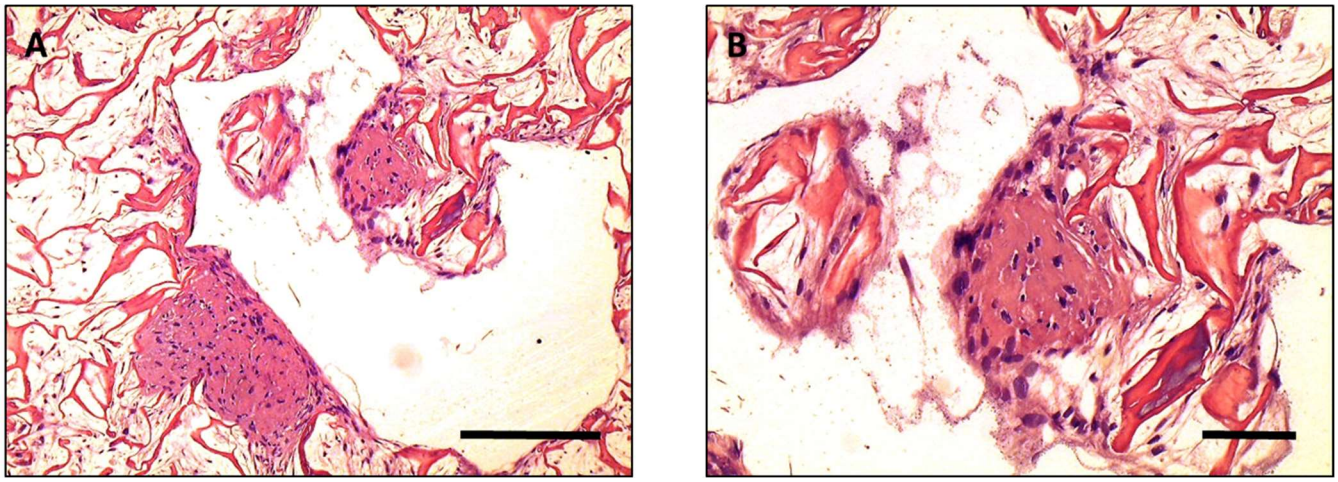

Figure 15: HN14 images of histological sections of the 3D primary culture at (A) 10X magnification (scale bars: 100 µm) and (B) 20X magnification (scale bars: 50 µm). The samples were stained with H&E.

We extracted the total mRNA from healthy and tumor tissues and measured the expression of vimentin (VIM), CDH1, CXCR4, TP53, TGFβ, MMP2 and MMP9 (Figure16 A and B). The comparison between the gene expression of HN2 and HN14 normal and malignant tissues showed higher levels of VIM (0.7 and 2.1), CXCR4 (1.4 and 2.8), TP53 (0.9 and 1.4) and MMP9 (17.9 and 4.7).

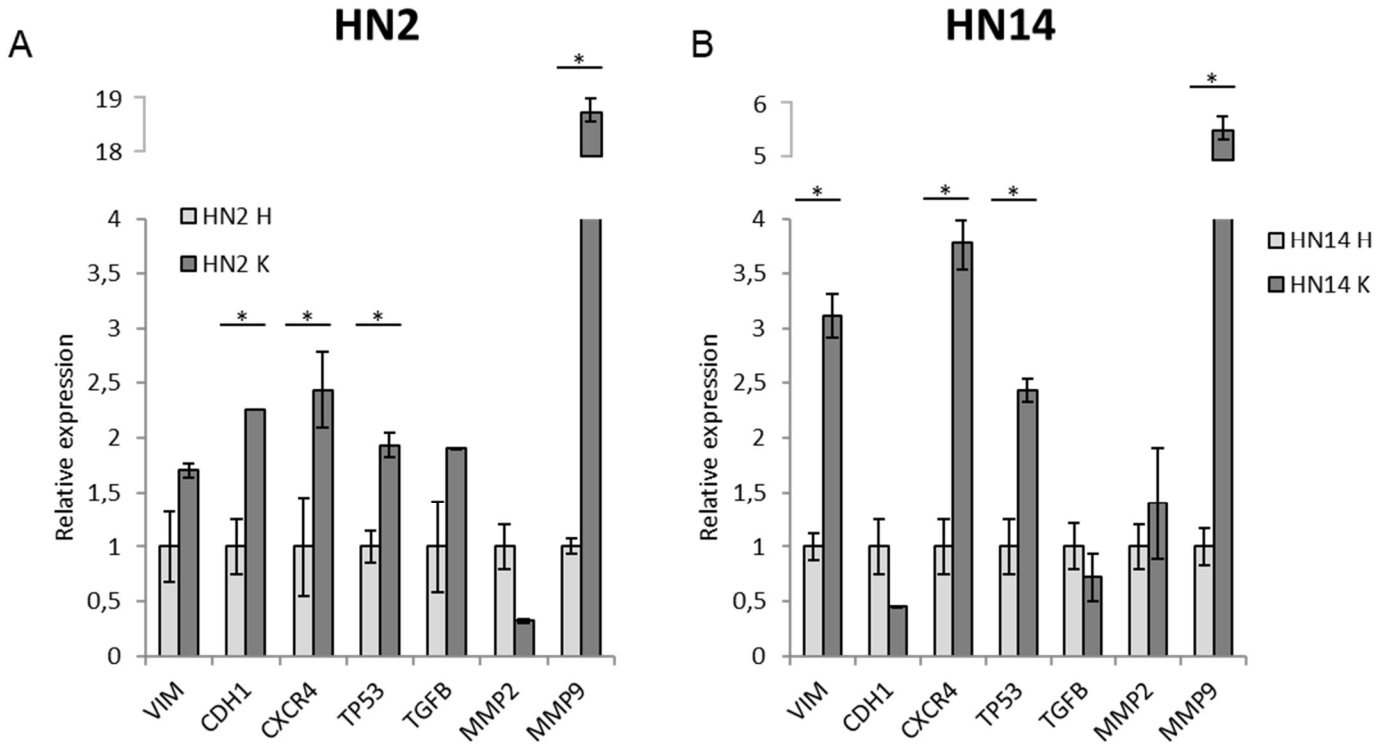

Figure 16: HN2 and HN14 relative expression of genes involved in tumor processes. (A,B) Gene expression of VIM, CDH1, CXCR4, TP53, TGFβ, MMP2 and MMP9 in malignant tissues (HN2 K and HN14 respectively) versus healthy tissues (HN2 H and HN14 H respectively). Data represent mean±S.D. (*) $p < 0.05$, two-tailed Student's t-test.

We have quantified the number of live/dead cells after the scaffold digestion with TDK on HNSCC cell lines. After 48h, the HNSCC cell lines displayed differences between 2D and 3D samples (Figure 17 A-L, and Table 3). All 2D cultures maintained high number of live cells (over 92%) after the recovery and staining. On the other hand, 3D cultures showed heterogeneous percentages of live cells. The cytofluorimetric analysis detected only the 13,82 % and 11,20 % of the total cells recovered for SCC15 and SCC25 cell lines, respectively Figure 17 C-D and E-F. The SCC90 and SCC152 3D cultures showed percentages of live cells under the 50% (respectively Figure 17 G-H and I-J). Due to the low level of viable cells obtained after the digestion with TDK, we have selected the two cell lines that displayed the higher value of live cells, SCC6 (63,84 %) (Figure 17 A-B) and SCC154 (89,91 %) (Figure 17 K-L).

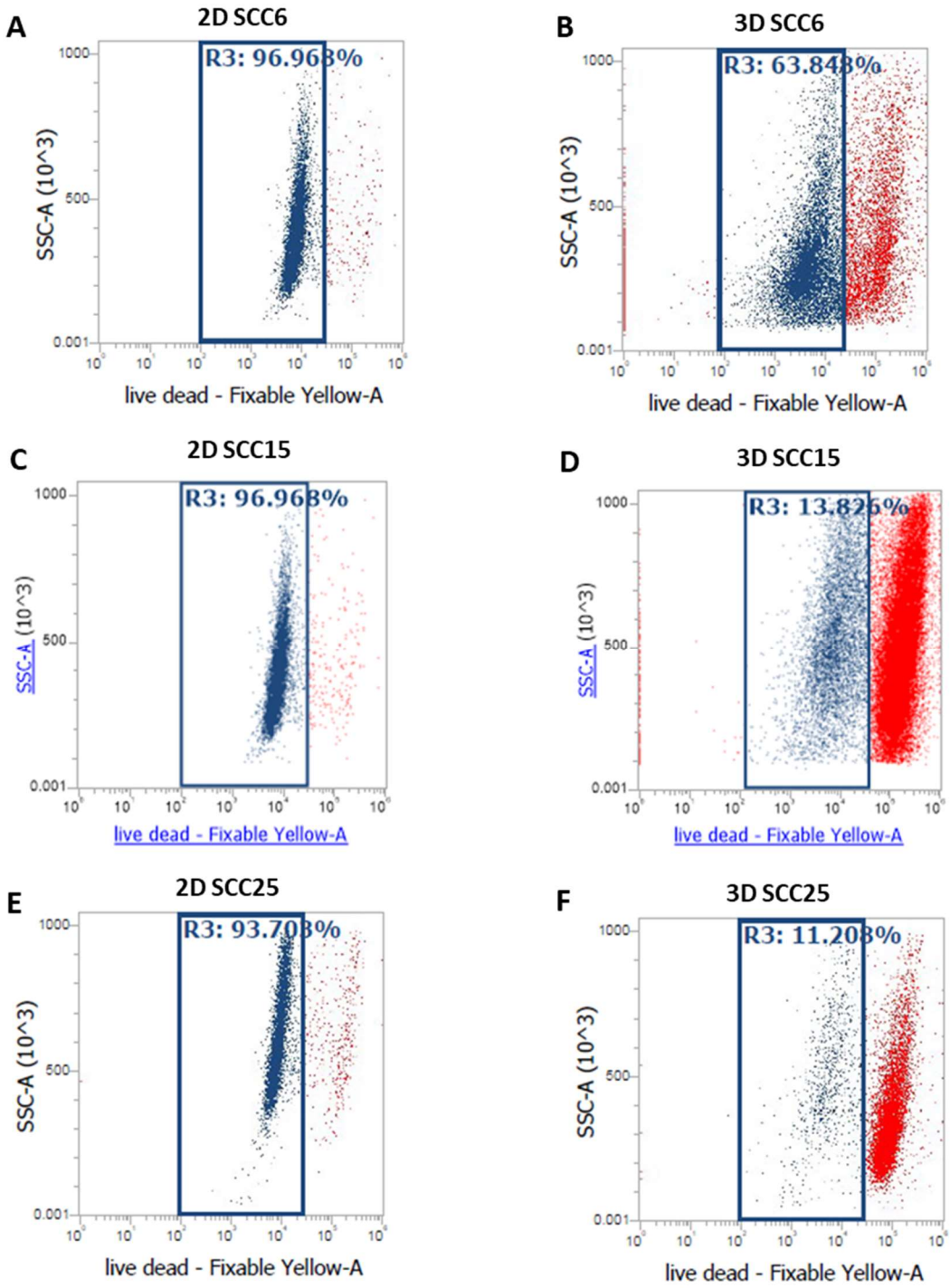
A
2D SCC6
R3: 96.968%
SSC-A (10^3)
live dead - Fixable Yellow-A
B
3D SCC6
R3: 63.848%
SSC-A (10^3)
live dead - Fixable Yellow-A
C
2D SCC15
R3: 96.968%
SSC-A (10^3)
live dead - Fixable Yellow-A
D
3D SCC15
R3: 13.826%
SSC-A (10^3)
live dead - Fixable Yellow-A
E
2D SCC25
R3: 93.708%
SSC-A (10^3)
live dead - Fixable Yellow-A
F
3D SCC25
R3: 11.208%
SSC-A (10^3)
live dead - Fixable Yellow-A

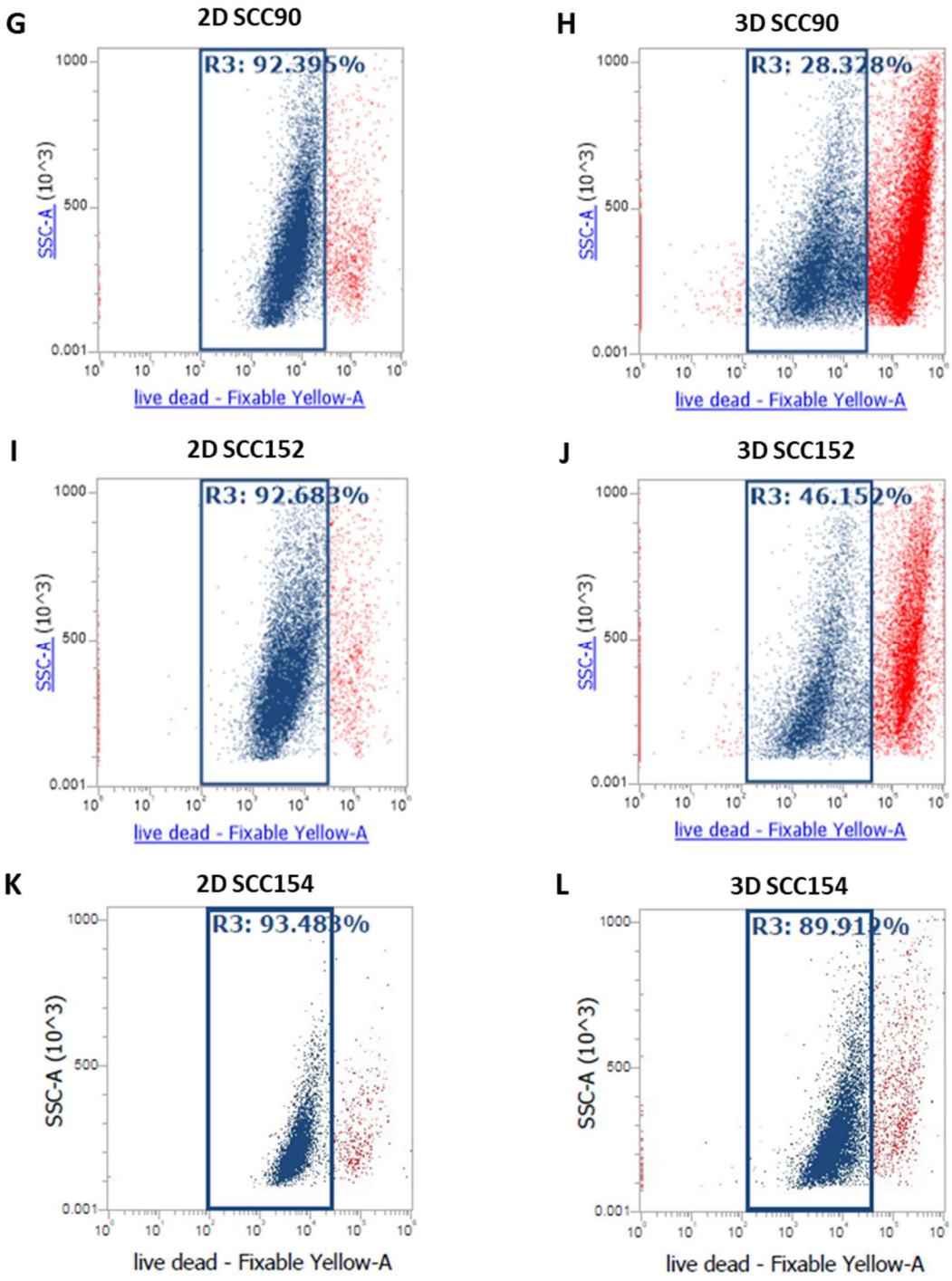

Figure 17 A-L: Representative dot plots of the percentage of live HNSCC cells after recovery in 2D and 3D cultures at 48h post seeding.

	2D	3D
SCC6	96,96	63,84
SCC15	96,96	13,82
SCC25	93,7	11,2
SCC90	92,39	28,32
SCC152	92,68	46,15
SCC154	93,48	89,91

Table 3: Percentage of viable cells in 2D and 3D HNSCC cultures

4.3 The scaffold microenvironment induces different hypoxic and proliferative area distribution

In order to explore the feature of the scaffold microenvironment, we have used immunohistochemical staining to detect the expression of HIF1-α, a regulator of cellular and developmental response to hypoxia. We analyzed slices of SCC6 and SCC154 3D cultures at 48h after seeding. Both cell lines displayed high positivity for HIF1-α in all the scaffold area (Figure 18).

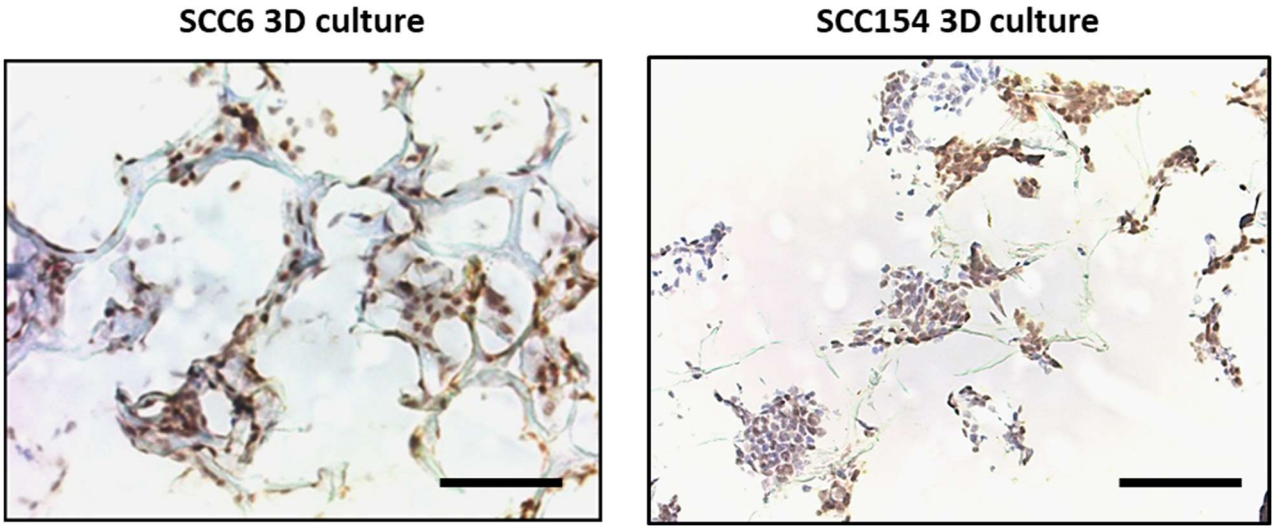

Figure 18: Representative images of HIF-1α stained SCC6 and SCC154 cells in histological sections of 3D cultures. Brown spots represented HIF-1α positive cells. Scale bar: 50 µm.

Then, we have studied the cell proliferation inside the scaffold area by a spatial point of view. We have performed a transfection with a lentiviral system to introduce FastFUCCI transgenes into our HNSCC cell lines. The fluorescence ubiquitination-based cell cycle indicator (FUCCI) induced the expression of different fluorescent proteins based on the phase of cell cycle. The cell engineering method failed in SCC15, SCC90 and SCC152 cells. One the other hand, the transfection protocol worked correctly on SCC6, SCC25 and SCC154 cell lines.

We started to test if the transfection process has altered the viability of the cell lines. No significant differences were detected between the transfected and non-transfected cells except for SCC154 and SCC154-FUCCI at 7 days post seeding (Figure 19).

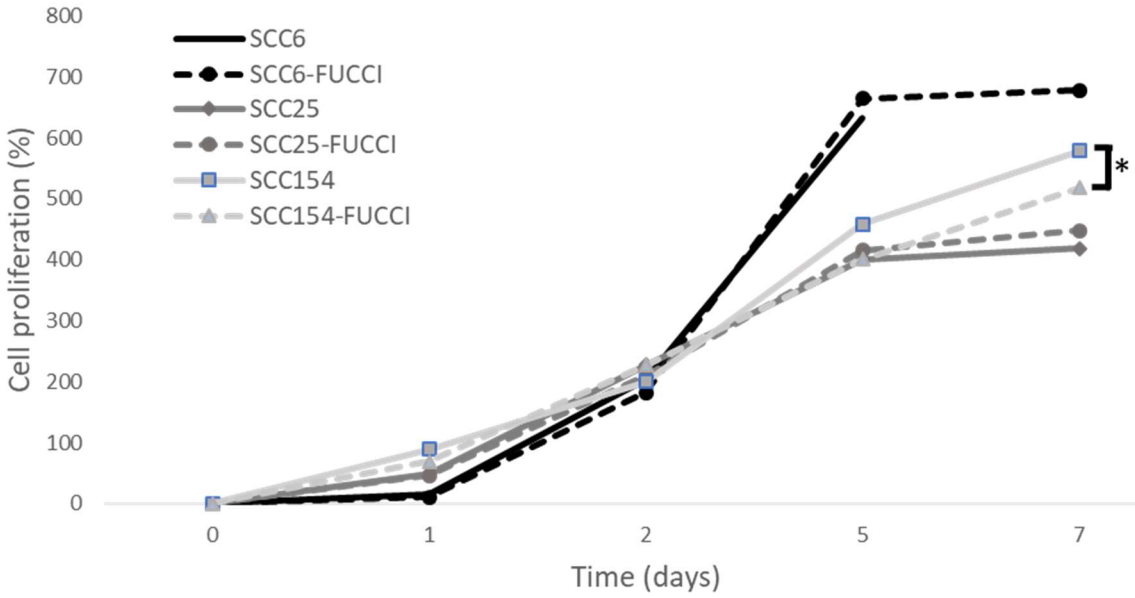

Figure 19: Fold changes in percentage of cell proliferation (relative to day 0) of HNSCC cell lines transfected and un-trasfected with FUCCI after: 1, 2, 5 and 7 days.

We have analyzed 8 images per conditions, 4 in the edge area and 4 in the core area of the scaffold, counting the red (G1 phase) and green cells (S/M-G2 phase) (Figure 20).

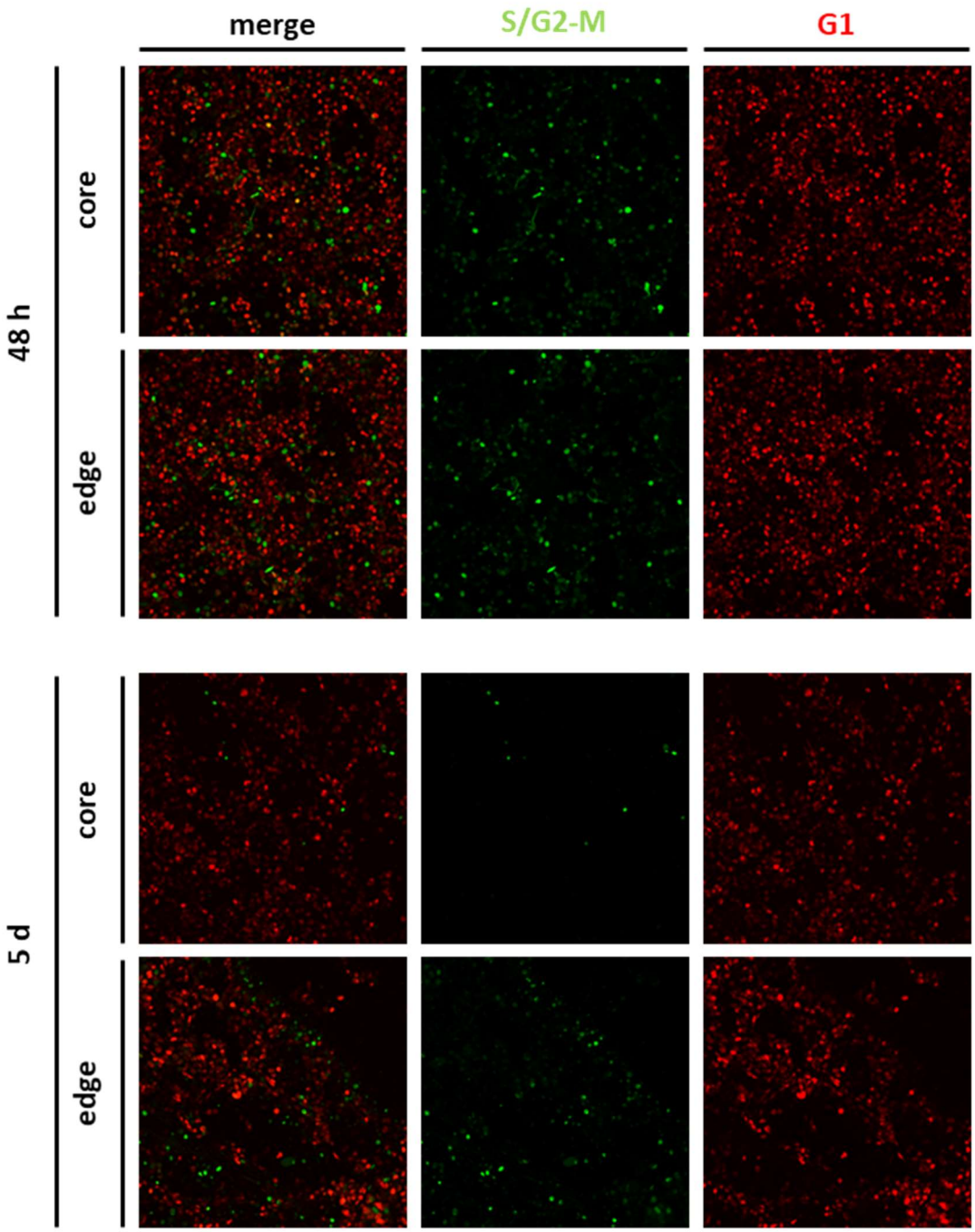

Figure 20: Representative images of HNSCC cells transfected with FastFUCCI plasmid in 3D culture at 48h and 5 days post seeding. Green and red spots represent cells in S/M-G2 and G1 phase respectively.

The results on SCC6 and SCC154 cell lines were homogenous. No differences were observed between the two regions at 0h and 5 days post seeding. At 48h, the cells in the edge area of the scaffold maintained an active proliferation behavior while in the core regions the number of cells in G1 phase increased. This condition was the same for SCC6 and SCC154 cell lines (Figure 21 and 22). The difference in S/G2-M cell percentage is significant between the edge and core only at 48h. At 5 days post-seeding this difference becomes not significant.

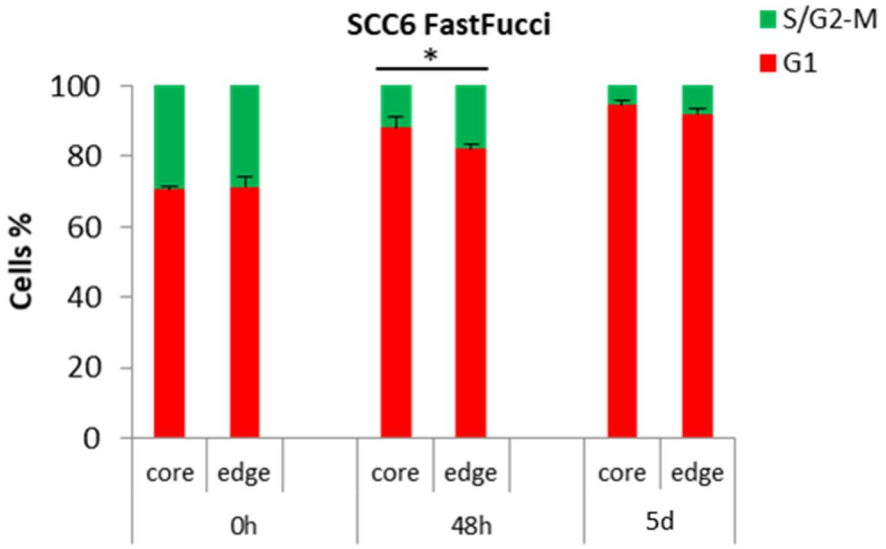

Figure 21: Percentage of SCC6-FUCCI cells in G1 or S/G2-M phase.Image-based cell cycle profiling. Fractions of red and green cells were quantified using the Imagej software. The data were obtained in relation to the number of red spots (red bars) and green spots (green bars).

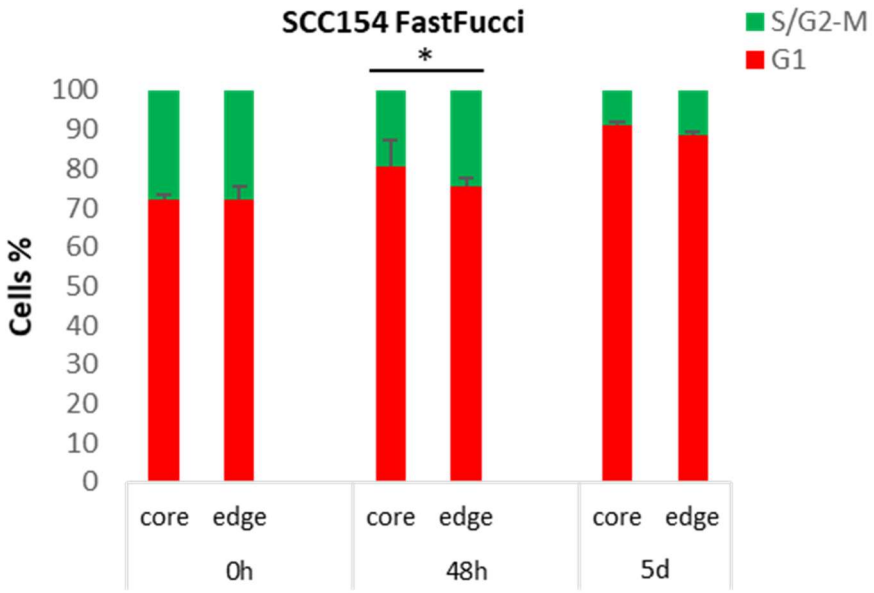

Figure 22: Percentage of SCC154-FUCCI cells in G1 or S/G2-M phase.Image-based cell cycle profiling. Fractions of red and green cells were quantified using the Imagej software. The data were obtained in relation to the number of red spots (red bars) and green spots (green bars).

4.4 Drugs sensitivity of 2D and 3D cultures

We studied the effect of drugs used in clinical practice and agents targeting monocytes and macrophages. The first molecules tested represented the first and second line chemotherapy treatments: cisplatin (CIS), 5' fluorouracil (5-FU), and gemcitabine (GEM). Concentrations were selected based on the plasma peak of each drug. The 2D and 3D cultures were treated with 0.1, 1 and 10 times the plasma peak concentration.

Both cell lines displayed higher sensibility for each drug when cultured in 2D supports respect the scaffold devices (Figure 23 A-C). Differently, monocytes showed the opposite behavior at the higher concentration with differences in survival percentage of 13.5, 43 and 53.8 between 2D and 3D cultures. The same drug sensibility profile was detected for monocytes treated with gemcitabine plasma peak.

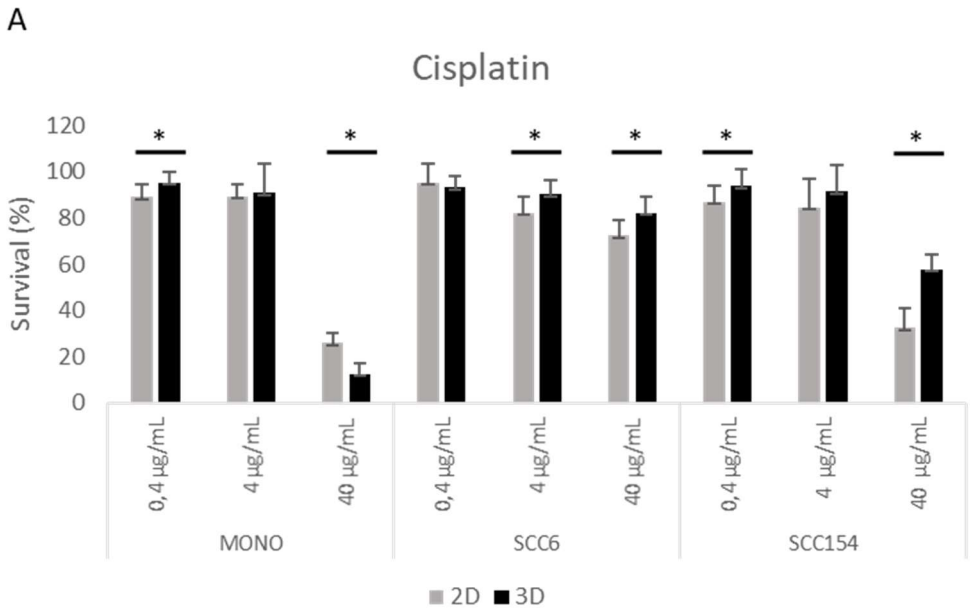

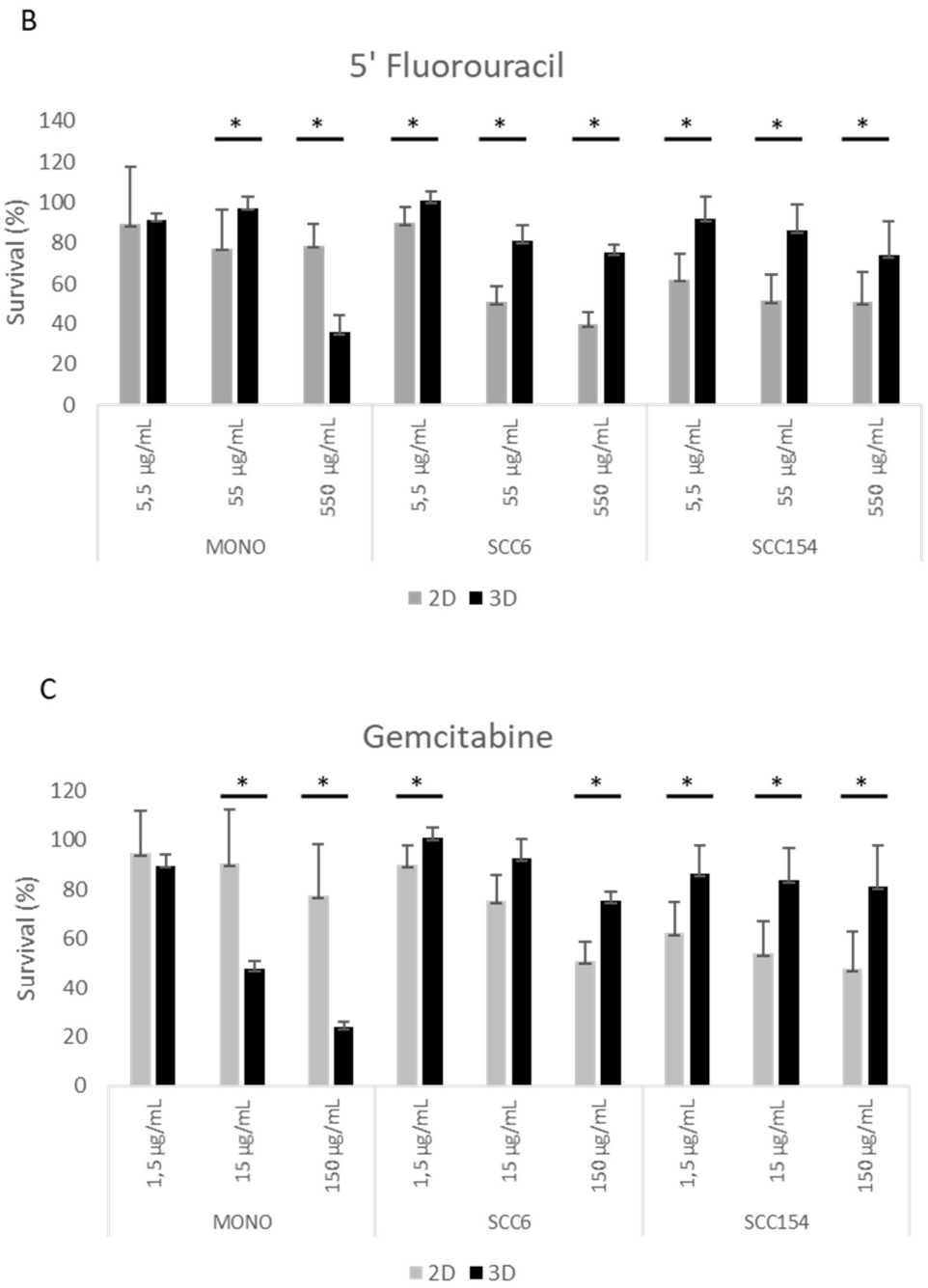

Figure 23: Cytotoxicity analysis of Monocytes (MONO), SCC6 and SCC154 cell lines treated with (A) Cisplatin, (B) 5' Fluorouracil and (C) Gemcitabine. Differences between 2D and 3D cultures were assessed by a 2-tailed Student's t-test and accepted as significant (*) at $P < 0.05$.

Currently, immunotherapy represents the first line treatment for HNSCC patients. For this reason, we tested the effect of Nivolumab and Pembrolizumab on 2D and 3D culture with the same approach used for chemotherapeutic agents (Figure 24 A and B).

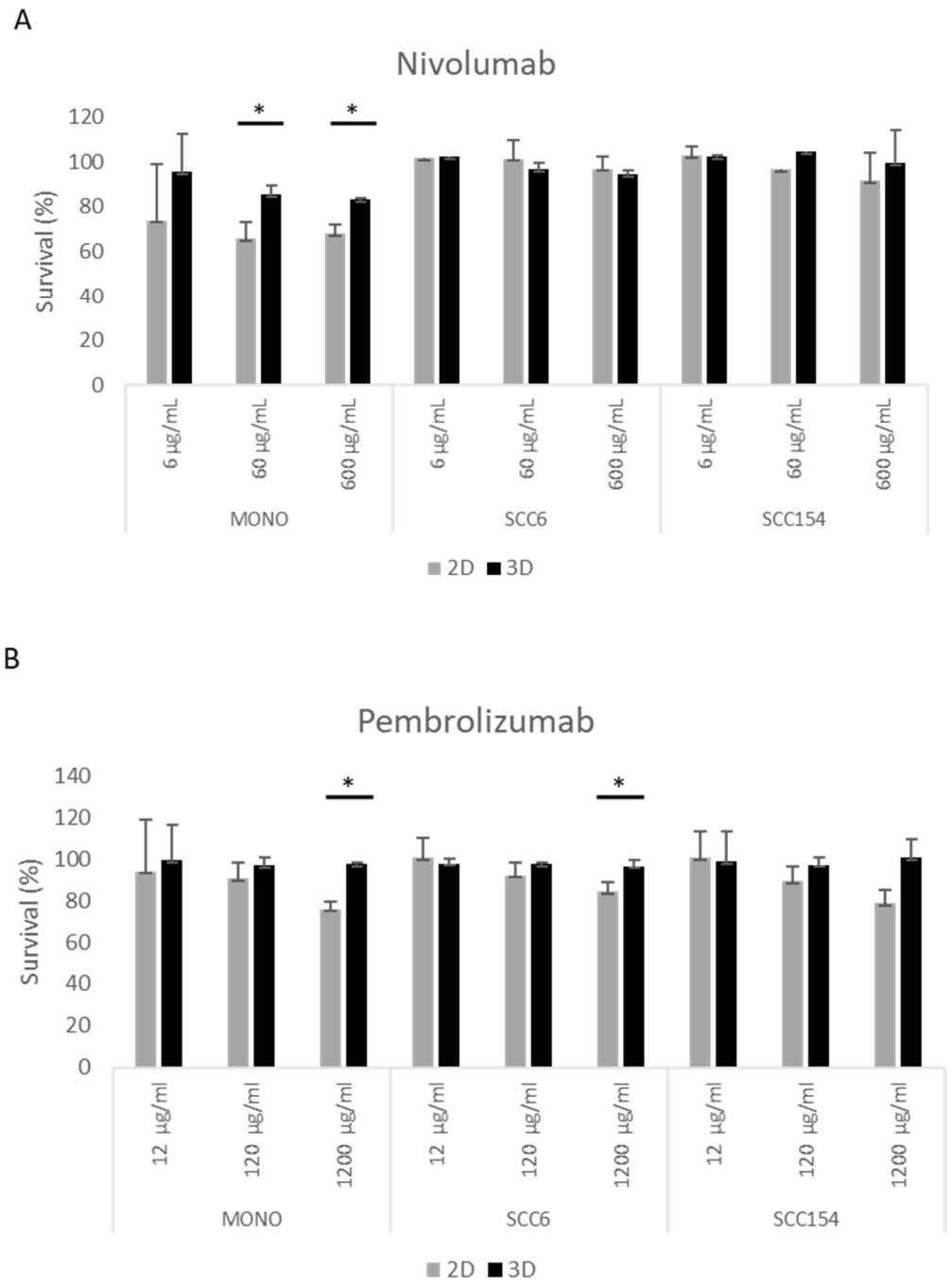

Figure 24: Cytotoxicity analysis of Monocytes (MONO), SCC6 and SCC154 cell lines treated with (A) Nivolumab and (B) Pembrolizumab. Differences between 2D and 3D cultures were assessed by a 2-tailed Student's t-test and accepted as significant (*) at $P < 0.05$.

The two cancer cell lines did not display significant differences except for the SCC6 treated with 1200 µg/mL. 3D monocytes culture showed higher sensibility to the higher concentration and at the Nivolumab plasma peak.

The last treatment tested was Trabectedin, a drug that have displayed a strong effect on monocyte and macrophage cell populations (Figure 25).

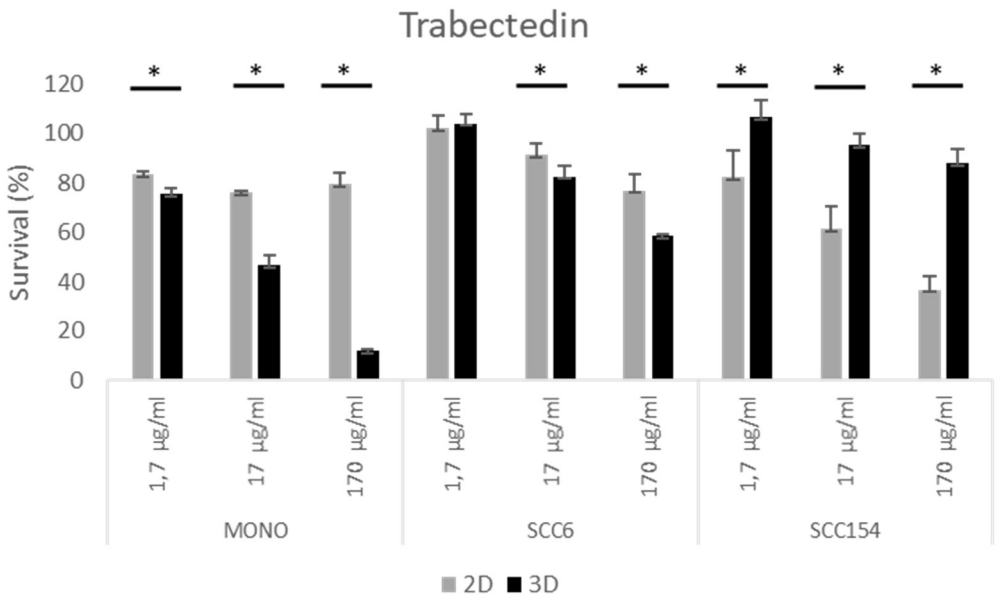

Figure 25: Cytotoxicity analysis of Monocytes (MONO), SCC6 and SCC154 cell lines treated with Trabectedin. Differences between 2D and 3D cultures were assessed by a 2-tailed Student's t-test and accepted as significant (*) at $P < 0.05$.

The SCC154 cells displayed the same behavior of the other treatments. Differently, SCC6 3D cultures were more sensitive to Trabectedin respect 2D counterparts for 17 and 170 µg/mL concentrations and the same effect were detected in all the monocytes conditions with differences up to 67.8 % of survival between 2D and 3D cultures.

4.5 Characterization of HNSCC/Monocyte 3D coculture

The co-culture of tumor cells and monocytes was developed by considering the data obtained from the characterization of the relative monocultures. We used a ratio of 1:1 of the two cell populations at different time points. We left cancer cells in the scaffold for forty-eight hours in order to mimic the tumor mass. After forty-eight hours, we seeded the CD14+ monocytes in order to mimic the immune cells infiltration in the TME (Figure 26). The co-culture was maintained for other 48h because usually studies on the effect of soluble factors on monocyte differentiation need from 2 to 4 days to exert their effects.

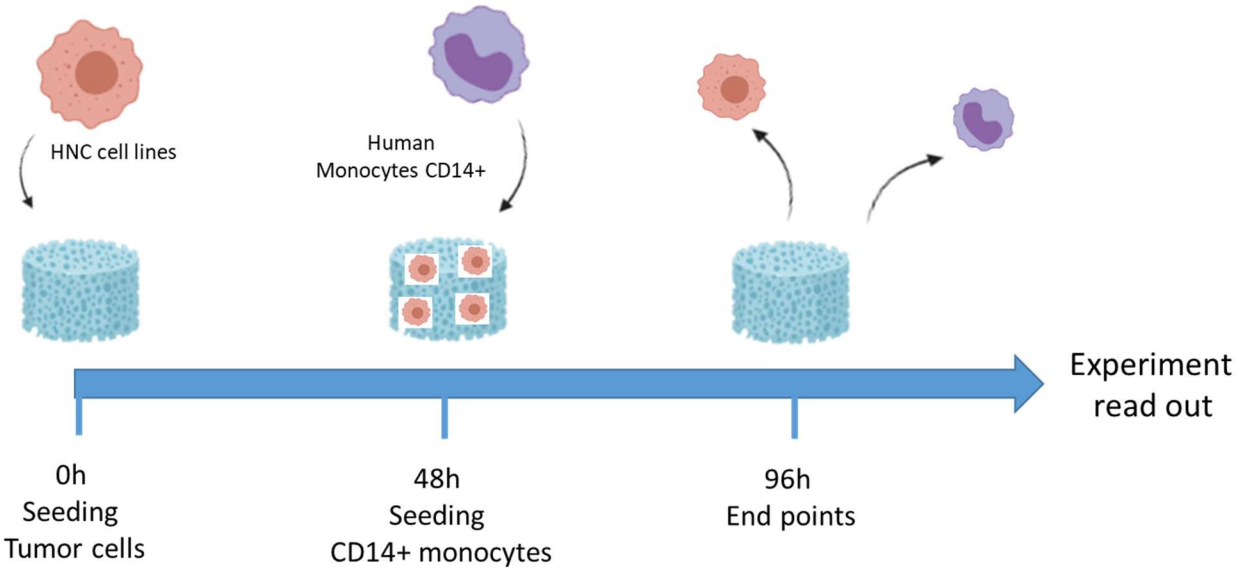

Figure 26: In vitro coculture experimental design.

The cell viability of tumor cells and monocytes recovered by the 3D co-culture was measured through cytofluorimetric analysis (Figure 27 A, B, D, E, G and H). The staining with CD14 and CD45 Ab was used to discriminate between the leukocyte population (CD14+/CD45+) and malignant cells (CD14-/CD45-) (Figure 27 C, F and I). The two distinct monocultures confirmed the high cell viability after the scaffold digestion (94.8 % and 78 % in monocytes and tumor cells respectively). This condition was maintained also in the co-culture system showing a percentage of viability of 93.2 %.

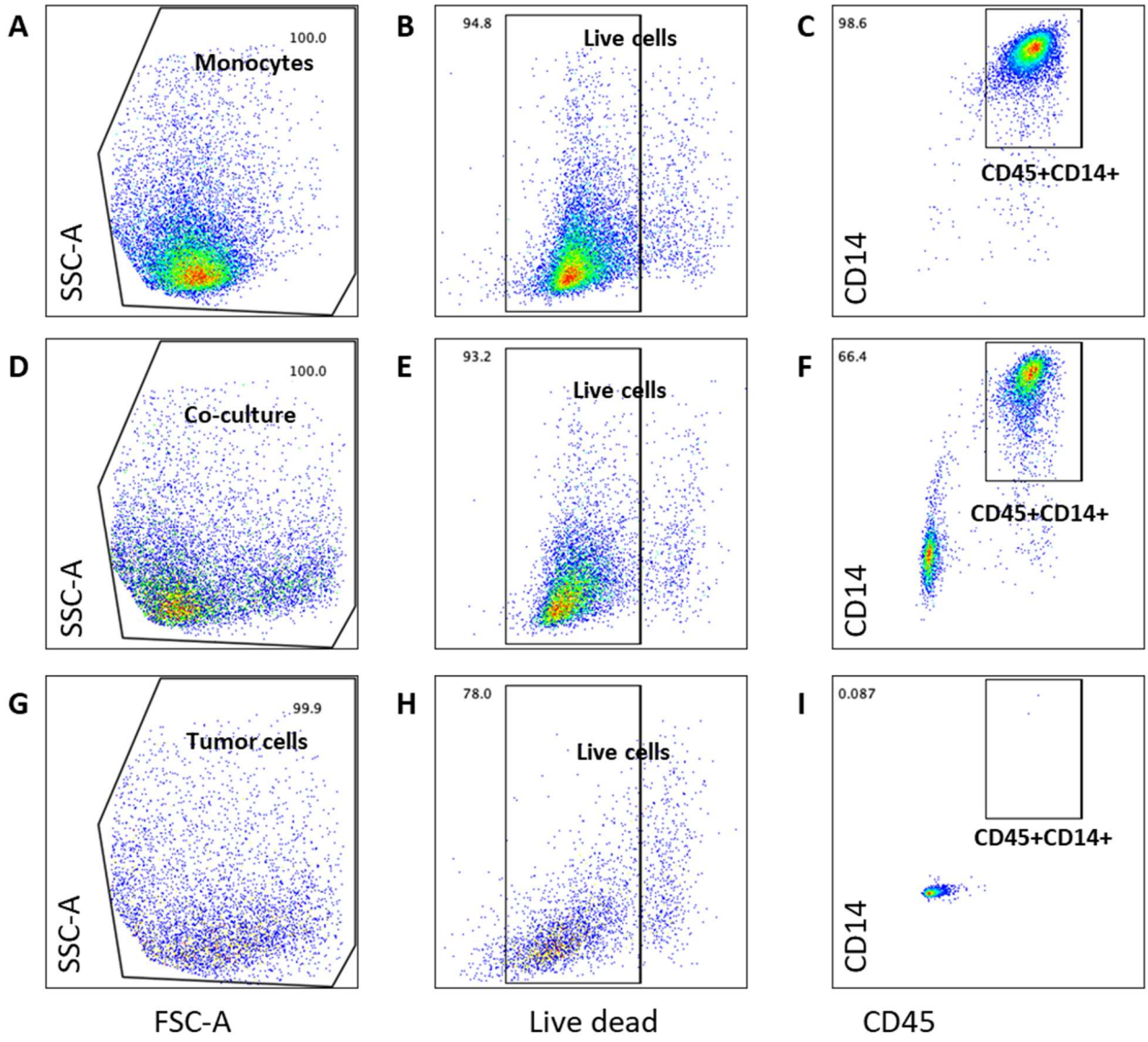

Figure 27: Representative morphologyc, live/dead and CD14/CD45 staining dot plots of: (A-C) monocytes monoculture, (D-F) monocyte/tumor cell coculture and (G-I) tumor cell monoculture. Spots inside the square plots in Figure D, G and J represent live cells. Spots inside the square plots in figure E, H and K represent cells positive for both CD14 and CD45 markers.

At this point, we tested the expression of macrophages markers to investigate the influence of the 3D structure and HNSCC cell lines on the monocyte polarization. Both cell lines induced low expression of PD-L1 and CCR7. Conversely, the SCC6 co-culture increased the number of cells HLA-DR^{+}/CD206^{+} up to 40 % of the whole population (Figure 28).

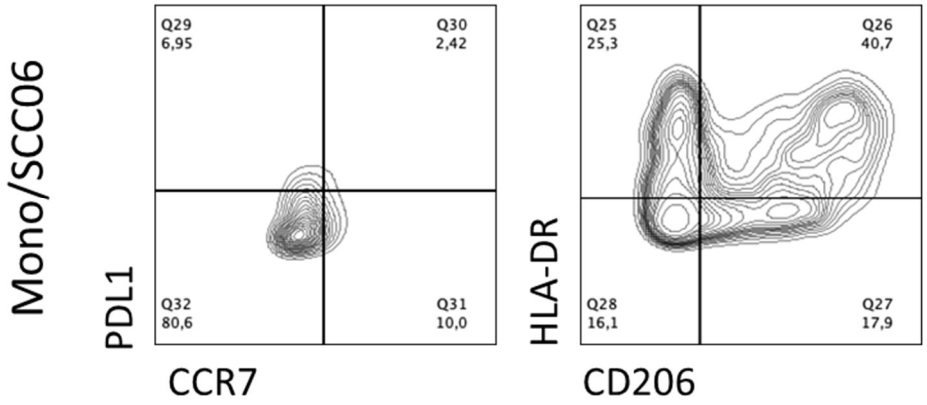

Figure 28: Representative M1 (CCR, HLA-DR) and M2 (PDL1, CD206) macrophages differentiation markers staining dot plots of 3D monocytes/SCC6 coculture. The different area report the percentage of cells: negative for each markers (lower left), CCR7 or CD206 positive (lower right), PDL1 or HLA-DR positive (top left) and double positive (top right).

SCC154 cells induced the expression of the same markers but the number of double positive cells was lower, about 23.1 % (Figure 29).

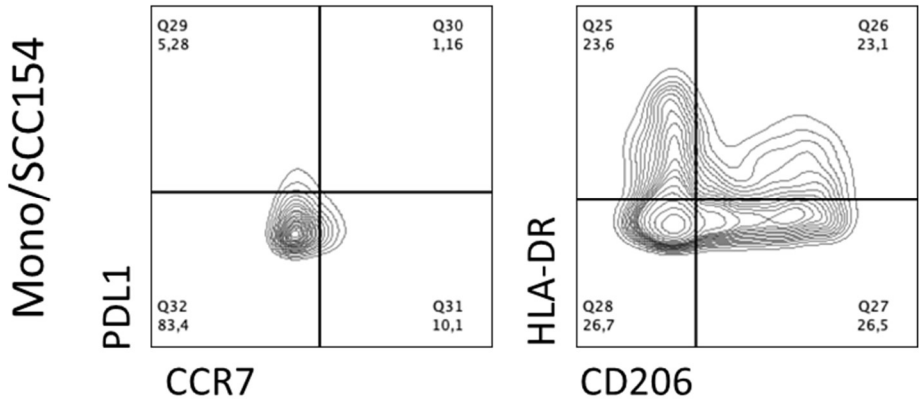

Figure 29: Representative M1 (CCR, HLA-DR) and M2 (PDL1, CD206) macrophages differentiation markers staining dot plots of 3D monocytes/SCC154 coculture. The different area report the percentage of cells: negative for each markers (lower left), CCR7 or CD206 positive (lower right), PDL1 or HLA-DR positive (top left) and double positive (top right).

Based on the expression of M2 macrophages markers showed by monocytes in the 3D cocultures, we studied the phagocytosis processes with confocal microscopy and cytofluorimetric technology. 3D images of cocultures showed Orange CMRA-labeled monocytes/macrophages (yellow) phagocytized Deep Red-labeled cancer cells (Figure 30).

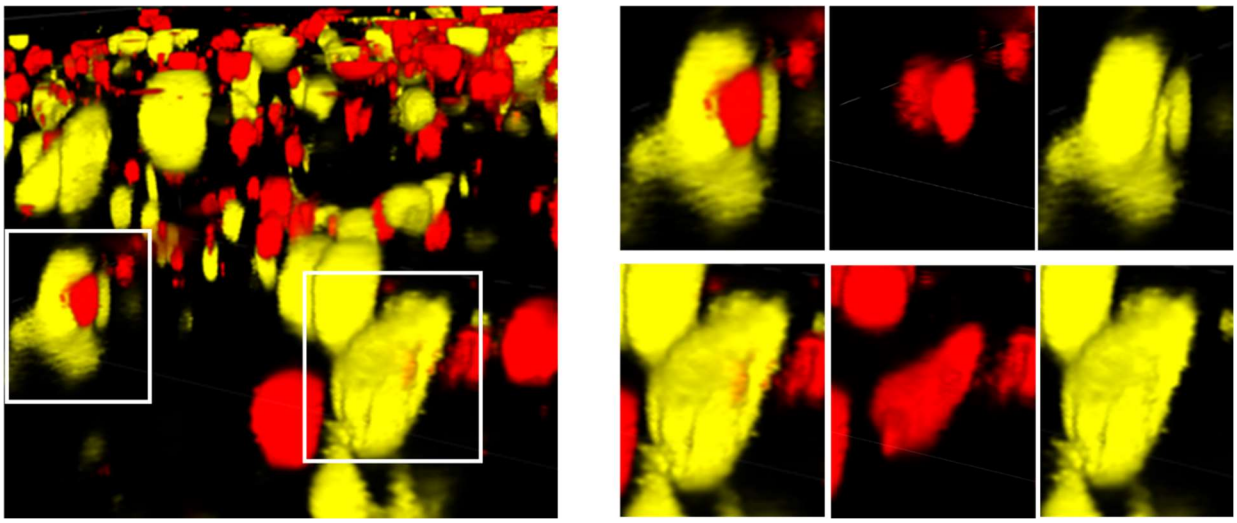

Figure 30: Confocal microscopy representative images of 3D co-culture with Orange CMRA-labeled monocytes (yellow) and CM-Dil-labeled SCC6 cells (red).

5. Discussion

In recent years, the incidence of HNSCCs has been increasing, with potential changes in associated risk factors due to the decrease of smoking, especially in developed countries [145]. Until recently, the studies on head and neck carcinogenesis were mainly focused on the cancer cell features, such as phenotype, mutation status, transcriptomic, etc. Given the aggressiveness, the therapy resistance and immunosuppression, the biological complexity of these cancers cannot be described only by cancer cells features. In this context, new important actors have been taken into consideration to deeply explore cancer behaviors. In particular, most of the tumor processes, such as progression, drug response and metastasis development, are influenced by TME components and composition [146]. The tumor niche structure is composed by a fibrous matrix produced by the TME cell components, and it is rich in metabolites, hormones, and growth and paracrine factors. These conditions induce the selection of the most aggressive tumor subclones and make the TME a supportive and favorable milieu for cancer growth and metastasis [147]. Moreover, cell populations that compose the TME, such as vascular endothelial cells, fibroblast, mesenchymal cells and hemopoietic derived immune cell populations, contribute to support the tumor progression. Due to the implementation of immunotherapy for the treatment of HNSCC patients, the interest in studying the immune system role in cancer has been increased in last years. The current knowledge of the role of immune cell populations in cancerogenesis and response to therapies represent remarkable achievements of anticancer medicine. Although the main role of T cells in immunotherapy response, it is not clear yet if the other immune cell populations have a role in this process. Among these, it is well known the correlation between the presence of macrophages in the TME and a bad prognosis [148].

In this context, we have decided to study the crosstalk between monocytes, macrophages and HNSCC cells in a 3D microenvironment. Through the combination of co-cultures and 3D devices, we aimed to develop an innovative approach to study the crosstalk between immune cells and cancer cells. Indeed, the development of an in vitro tumor niche that reproduce all the cellular and acellular components of the TME is still utopic. We adopted the strategy to integrate different validated models to study and predict cancer behaviors though a reliable biomimetic system.

The 3D model selected for this study is represented by a collagen-based biomimetic scaffold. This device is composed by fibers of bovine collagen type I that have been organized in a 3D porous structure through a freeze-drying process. The collagen scaffold biophysical properties were already described in a previous study published in 2017 [148]. The device macrostructure was 2 mm of mean thickness and 9 ± 0.5 mm of mean diameter. The pores size was described in a range between 150 and 300 μm, with a mean pore dimension of 197 ± 25 μm. The collagen type I was selected for the scaffold synthesis because it is one of the main ECM protein in every tissue. In this context, we used collagen-based scaffolds as a “tissue-like” support for the cells’ growth in a biomimetic 3D microenvironment.

The first part of the project has been focused on the identification of the best culture conditions for mono- and co-cultures. In the last years, we have used this *in vitro* system to study the interaction between the 3D structure and monoculture of breast and oropharynx cancer cells [128,130]. Malignant cells were already cultured on this kind of system, but it is the first time in literature that monocytes have been seeded on a collagen-based scaffold. Moreover, the human monocytes represent a kind of cell population more difficult to manage compared to immortalized cell lines due to the human origin and their non-proliferating nature. For these reasons, we tested different culture media and cell concentrations to identify the conditions that allow the highest monocytes viability. In our previous studies on breast and H&N cancers, we seeded 5 and 3,5 x 10^6 cells per scaffold, respectively. Based on literature evidence showing an estimated 1:1 ratio of monocyte and tumor cells in H&N cancer tissues [6], we have chosen as first option the half of cells concentration used in the two previously studies, in order to obtain a future co-culture reflecting the real features of the tumor microenvironment. The selection parameters have been based on the viability of monocytes. Safi W. et al. described the in vitro management of monocyte with different culture conditions [150]. Regardless the media used, monocytes increased the cell viability from day 1 to 7. We confirmed the data in 2D but, surprisingly, the same behavior was shown by the 3D conditions. Conversely, all the six cell lines of HNSCC decreased the viability from day 1 to 5. Moreover, only a small portion of the total number of monocytes was lost for cell death or loss of adhesion to the collagen fibers. All these aspects demonstrate a good tolerance of monocytes to the 3D microenvironment and to the culture parameters selected, even more than cancer cell lines.

The cell recovering from 3D scaffolds represents an important experimental phase as most of in vitro and in vivo technologies need single cell suspensions to be performed. One of the options is the matrix digestion through chemical, enzymatic or mechanical approaches. These protocols can be stressful for cells and decrease the viability of the sample. We tested different protocols using monocytes 3D monocultures to select the most efficient mechanical and enzymatic digestion protocol for the recovery of monocytes by considering the number of cells recovered, and viability percentage. The data obtained on the HNSCC cell lines displayed high heterogeneity in term of viability. Indeed, the protocol resulted effective for the recovery of two cell lines (SCC6 and SCC154), but inefficient for the other samples. Although the cells viability of the six cell lines decreased in a range from 10 % to 30 % at 48h post seeding, the live cells obtained after recovery displayed percentage of viability between 10 and 90. Therefore, the mechanical and enzymatic protocol identified cannot be applied for all the cell types, but have to be modified according the sample analyzed.

The decrease in viability showed by cancer cells can be justified by the microenvironment features of the scaffold. Indeed, our previously studies demonstrated the development of a hypoxic core in the inner area of the device [128,130]. We confirmed this condition also in the 3D monoculture of the two HNSCC cell lines used in the project. Low level of oxygen affects many biological processes, including cell cycle and proliferation. Therefore, we have evaluated if the 3D microenvironment was able to modulate these aspects.

As previously reported, the proliferation analysis of the six cell lines displayed for each sample the exponential growth phase typical of cancer cells growth in 2D monolayer supports. On the other hand, al the cancer 3D cultures showed a constant decrease of the viability. Moreover, spatial analysis of the cell cycle in the core and edge areas of the scaffold identified different behaviors. High levels of oxygen and nutrients in the peripheral of the device induced a higher level of cell proliferation compared to the inner area. Thus, this model perfectly recapitulates the spatial structure typical of the tumor mass organized in a necrotic core surrounded by proliferative cell populations.

All the data collected were used as starting point for the characterization of the co-culture model. The cell concentrations and media selected for the monoculture of monocytes and HNSCC cancer cells did not modify the viability of co-cultured cells. These culture parameters make our model suitable to study the role of the ECM and malignant components on the immune cells phenotypic and genotypic features.

Monocytes are the class of leukocytes that can differentiate into macrophages. These cells can acquire different polarization with opposite functions, M1 macrophages with an anti-inflammatory action and M2 macrophages supporting the inflammatory signaling. We used collagen-based scaffold as a biomimetic model to study the influence of the 3D structure on the monocyte maturation and polarization. We compared the expression of M1 (HLA-DR and CCR7) and M2 (CD206 and PD-L1) macrophages markers in 2D and 3D cultures. The monolayer model drove monocytes to M1 polarization through the expression of high levels of HLA-DR and CCR7 while the cells were negative for M2 macrophage markers. Differently, the 3D culture microenvironment induced the expression of CD206 and lower level of HLA-DR. The two models seemed to stimulate distinct differentiation profiles due to different microenvironment characteristics. The scaffold structure promoted the expression of M2 markers and decreased the M1 counterparts. This effect can be explained by the action of the hypoxic core present in the inner part of the device, as low level of oxygen promoted the M2 macrophages polarization [151,152]. Thus, the microenvironment features of the collagen-based scaffold would be able to drive monocytes towards the differentiation in pro-inflammatory macrophages.

If we added to the model the variable of cancer cell populations, the monocytes phenotype further changed. Both cell lines used to develop the co-culture system induced the differentiation of two population of monocytes with different proportions. Indeed, the cytofluorimetric analysis showed a new population HLA-DR^+/$CD206^+$ not present in the monoculture models. Moreover, the expression of CD206 increased significantly. Interestingly, in the co-culture with the HPV negative cell line; this monocytes population was higher than in the HPV positive counterpart. Indeed, the HPV can induce the onset of these kind of tumor, although less aggressive than cancer developed by environmental and habit factors. Therefore, the more aggressive phenotype induced by the HPV negative cell lines reflects the clinical and biological evidence of these different diseases.

The project has identified the culture parameters to obtain a three-dimensional microenvironment suitable for the study of interaction between monocytes and tumor cells. We have used this model to describe growth dynamic, drug sensibility and phagocytosis processes influenced by the 3D structure. The main results are focused on the cultures characterization but furthered analysis are needed to study the effects of the this model on the crosstalk between immune components and HNC cells. We will sequencing the two populations in order to underline the transcriptomic alterations induced by the cell interactions and by the 3D microenvironment. Moreover, we will confirm the effect of the treatments observed in vitro on an in vivo model.

In conclusion, our biomimetic 3D model is suitable for cultures of monocytes and support their viability more than the classical monolayer supports. On the other hand, the device microenvironment is not compatible for the growth of all HNSCC cell lines, although it is able to reproduce spatial areas with different biophysiological characteristics typical of the tumor mass. Moreover, the 3D collagen-based scaffold induces the expression of M2 macrophages markers, an effect increased by the addition of cancer cell lines. All these results make our biomimetic 3D device a promising in vitro tool to increase the reliability of in vitro studies on the interaction between ECM, immune and cancer cells.

6. References

[1] Barsouk A et al. Epidemiology, Risk Factors, and Prevention of Head and Neck Squamous Cell Carcinoma. Med Sci (Basel). 2023 11(2):42. doi: 10.3390/medsci11020042.

[2] Chow Q.M.L. Head and Neck Cancer. N Engl J Med. 2020, 382, 60-72. doi: 10.1056/NEJMra1715715.

[3] Sanderson R.J. et al. Squamous cell carcinomas of the head and neck. BMJ. 2002, 325, 822-7. doi: 10.1136/bmj.325.7368.822.

[4]] Kian Ang, K. et al. Human papillomavirus and survival of patients with oropharyngeal cancer. N Engl J Med. 2010, 363, 24-35. doi: 10.1056/NEJMoa0912217.

[5] Chen Y.P. et al. Nasopharyngeal carcinoma. Lancet 2019, 394, 64-80. doi: 10.1016/S0140-6736(19)30956-0.

[6] Johnson D.E. et al. Head and neck squamous cell carcinoma. Nat Rev Dis Primers. 2020, 6(1):92. doi: 10.1038/s41572-020-00224-3.

[7] Sung H. et al. Global Cancer Statistics 2020: GLOBOCAN Estimates of Incidence and Mortality Worldwide for 36 Cancers in 185 Countries. CA Cancer J Clin. 2021 71(3):209-249. doi: 10.3322/caac.21660.

[8] Hashibe M. et al. Interaction between tobacco and alcohol use and the risk of head and neck cancer: pooled analysis in the International Head and Neck Cancer Epidemiology Consortium. Cancer Epidemiol Biomarkers Prev. 2009, 18, 541-50. doi: 10.1158/1055-9965.EPI-08-0347.

[9] Sabatini M.E. et al. Human papillomavirus as a driver of head and neck cancers. Br J Cancer 2020, 122, 306–314. doi: 10.1038/s41416-019-0602-7.

[10] Benson E. et al. The clinical impact of HPV tumor status upon head and neck squamous cell carcinomas. Oral Oncol. 2014 50(6):565-74. doi: 10.1016/j.oraloncology.2013.09.008.

[11] Lechner M. et al. HPV-associated oropharyngeal cancer: epidemiology, molecular biology and clinical management. Nat Rev Clin Oncol. 2022 19(5):306-327. doi: 10.1038/s41571-022-00603-7.

[12] Miserocchi G. et al. Precision Medicine in Head and Neck Cancers: Genomic and Preclinical Approaches. J Pers Med. 2022 12(6):854. doi: 10.3390/jpm12060854.

[13] Kian Ang K. et al. Human papillomavirus and survival of patients with oropharyngeal cancer. N Engl J Med. 2010, 363, 24-35. doi: 10.1056/NEJMoa0912217.

[14] Chen Y.P. et al. Nasopharyngeal carcinoma. Lancet 2019, 394, 64-80. doi: 10.1016/S0140-6736(19)30956-0.

[15] Lee N.C.J. et al. Patterns of failure in high-metastatic node number human papillomavirus-positive oropharyngeal carcinoma. Oral. Oncol. 2018, 85, 35-39. doi: 10.1016/j.oraloncology.2018.08.001

[16] Forastiere A.A. et al. Use of larynx-preservation strategies in the treatment of laryngeal cancer: American Society of Clinical Oncology clinical practice guideline update. J. Clin. Oncol. 2018, 36, 1143-1169. doi: 10.1200/JCO.2017.75.7385.

[17] Bernier J. et al. Postoperative irradiation with or without concomitant chemotherapy for locally advanced head and neck cancer. N. Engl. J. Med. 2004, 350, 1945-52. doi: 10.1056/NEJMoa032641.

[18] Bauml, J.M. et al. Cisplatin every 3 weeks versus weekly with definitive concurrent radiotherapy for squamous cell carcinoma of the head and neck. J. Natl Cancer Inst. 2019, 111, 490-497. doi: 10.1093/jnci/djy133.

[19] Kitamura, N. et al. Current Trends and Future Prospects of Molecu-lar Targeted Therapy in Head and Neck Squamous Cell Carcinoma. Int J Mol Sci. 2020, 22, 240. doi: 10.3390/ijms22010240.

[20] Cramer, J.D. et al. Immunotherapy for head and neck cancer: Recent advances and future directions. Oral Oncol. 2019, 99, 104460. doi: 10.1016/j.oraloncology.2019.104460.

[21] Ribatti D. et al. The concept of immune surveillance against tumors. The first theories. Oncotarget. 2017 8(4):7175-7180. doi: 10.18632/oncotarget.12739.

[22] Zhang Y. et al. The history and advances in cancer immunotherapy: understanding the characteristics of tumor-infiltrating immune cells and their therapeutic implications. Cell Mol Immunol. 2020 17(8): 807–821. doi: 10.1038/s41423-020-0488-6

[23] Riley R.S. et al. Delivery technologies for cancer immunotherapy. Nat Rev Drug Discov. 2019 Mar; 18(3): 175–196. doi: 10.1038/s41573-018-0006-z

[24] Han Y. et al. PD-1/PD-L1 pathway: current researches in cancer. Am J Cancer Res. 2020 10(3): 727–742. eCollection 2020.

[25] Ai L. et al. Research Status and Outlook of PD-1/PD-L1 Inhibitors for Cancer Therapy. Drug Des Devel Ther. 2020 14:3625-3649. doi: 10.2147/DDDT.S267433.

[26] Shiravand Y. et al. Immune Checkpoint Inhibitors in Cancer Therapy. Curr Oncol. 2022 May; 29(5): 3044–3060. doi: 10.3390/curroncol29050247

[27] Park J.H. et al. Hyperprogressive disease and its clinical impact in patients with recurrent and/or metastatic head and neck squamous cell carcinoma treated with immune-checkpoint inhibitors: Korean

cancer study group HN 18-12. J Cancer Res Clin Oncol. 2020 146(12):3359-3369. doi: 10.1007/s00432-020-03316-5.

[28] Kobayashi K. et al. A Review of HPV-Related Head and Neck Cancer. J Clin Med. 2018 Sep; 7(9): 241. doi: 10.3390/jcm7090241

[29] Krishnamurthy S. et al. Endothelial cell-initiated signaling promotes the survival and self-renewal of cancer stem cells. Cancer Res. 2010, 70, 9969–9978. doi: 10.1158/0008-5472.CAN-10-1712.

[30] Reid P. et al. Diversity of cancer stem cells in head and neck carcinomas: The role of HPV in cancer stem cell heterogeneity, plasticity and treatment response. Radiother Oncol. 2019, 135, 1-12. doi: 10.1016/j.radonc.2019.02.016.

[31] Gillison M.L. et al. Distinct risk factor profiles for human papillomavirus type 16-positive and human papillomavirus type 16-negative head and neck cancers. J Natl Cancer Inst, 2008, 100, 407-420. doi: 10.1093/jnci/djn025.

[32] Vlashi E. et al. Radiation-Induced Dedifferen-tiation of Head and Neck Cancer Cells Into Cancer Stem Cells Depends on Human Papillomavirus Status. Int J Radiat Oncol Biol Phys, 2016, 94, 1198-206. doi: 10.1016/j.ijrobp.2016.01.005.

[33] Peitzsch C. et al. Cancer Stem Cells in Head and Neck Squamous Cell Carcinoma: Identification, Characterization and Clinical Implications. Cancers (Basel) 2019, 11, 616. doi: 10.3390/cancers11050616.

[34] Nör, C. et al. Cisplatin induces Bmi-1 and enhances the stem cell fraction in head and neck cancer. Neoplasia, 2014, 16, 137–46. doi: 10.1593/neo.131744

[35] Chen, A.M. et al. Re-duced-dose radiotherapy for human papillomavirus-associated squamous-cell carcinoma of the oropharynx: a single-arm, phase 2 study. Lancet Oncol, 2017, 18, 803-811. doi: 10.1016/S1470-2045(17)30246-2.

[36] Lee, J. et al. Ectopic overexpression of CD133 in HNSCC makes it resistant to commonly used chemotherapeutics. Tumor Biology, 2017, 39, 1010428317695534. doi: 10.1177/1010428317695534.

[37] The Cancer Genome Atlas Network. Comprehensive genomic characterization of head and neck squamous cell carcinomas. Nature 2015, 517, 576–582. doi: 10.1038/nature14129.

[38] Cerami E. et al. The cBio cancer genomics portal: an open platform for exploring multidimensional cancer genomics data. Cancer Discov. 2012, 2, 401–404. doi: 10.1158/2159-8290.CD-12-0095.

[39] Hecht S.S. et al. Smokeless tobacco and cigarette smoking: chemical mechanisms and cancer prevention. Nat Rev Cancer. 2022 Mar;22(3):143-155. doi: 10.1038/s41568-021-00423-4.

[40] Stein, A.P. et al. Prevalence of human papillomavirus in oropharyngeal cancer: a systematic review. Cancer J. 2015, 21, 138-46.

[41] Alsahafi, E. et al. Clinical update on head and neck cancer: molecular biology and ongoing challenges. Cell Death Dis. 2019, 10, 540.

[42] Zhou G. et al. TP53 Mutations in Head and Neck Squamous Cell Carcinoma and Their Impact on Disease Progression and Treatment Response. J Cell Biochem. 2016, 117, 2682-2692. doi: 10.1002/jcb.25592.

[43] Wiest T. et al. Involvement of intact HPV16 E6/E7 gene expression in head and neck cancers with unaltered p53 status and perturbed pRb cell cycle control. Oncogene 2002, 21, 1510-7. doi: 10.1038/sj.onc.1205214.

[44] Eckhardt M. et al. Multiple routes to oncogenesis are promoted by the human papillomavirus-host protein network. Cancer Discov. 2018, 8, 1474-1489. doi: 10.1158/2159-8290.CD-17-1018.

[45] Wilczyński JR. et al. Cancer stem cells in ovarian cancer-a source of tumor success and a challenging target for novel therapies. Int J Mol Sci. 2022 23:2496. doi: 10.3390/ijms23052496

[46] Wang C, et al. CD276 expression enables squamous cell carcinoma stem cells to evade immune surveillance. Cell Stem Cell. 2021 28:1597–613.e7. doi: 10.1016/j.stem.2021.04.011

[47] Qian X, et al. Biology and immunology of cancer stem(-like) cells in head and neck cancer. Crit Rev Oncol Hematol. (2015) 95:337–45. doi: 10.1016/j.critrevonc.2015.03.009

[48] Vannucci L. Stroma as an active player in the development of the tumor microenvironment. Cancer Microenviron. 2015 8(3):159–166. doi: 10.1007/s12307-014-0150-x.

[49] Bremnes R.M. et al. The role of tumor stroma in cancer progression and prognosis: emphasis on carcinoma-associated fibroblasts and non-small cell lung cancer. J Thorac Oncol. 2011 6(1):209–217. doi: 10.1097/JTO.0b013e3181f8a1bd.

[50] Naba A. et al. The matrisome: in silico definition and in vivo characterization by proteomics of normal and tumor extracellular matrices. Mol Cell Proteom. 2012 11(4):M111.014647. doi: 10.1074/mcp.M111.014647.

[51] Bergamaschi A. et al. Extracellular matrix signature identifies breast cancer subgroups with different clinical outcome. J Pathol. 2008 214(3):357–367. doi: 10.1002/path.2278.

[52] Otranto M. et al. The role of the myofibroblast in tumor stroma remodeling. Cell Adh Migr. 2012 6(3):203–219. doi: 10.4161/cam.20377.

[53] Garlanda C. et al. The interleukin-1 family: back to the future. Immunity. 2013 39(6):1003–1018. doi: 10.1016/j.immuni.2013.11.010.

[54] Dmitrieva OS, Shilovskiy IP, Khaitov MR, Grivennikov SI. Interleukins 1 and 6 as main mediators of inflammation and cancer. Biochemistry. 2016;81(2):80–90. [PubMed] [Google Scholar]

[55] Principe D.R. et al. TGF-β: duality of function between tumor prevention and carcinogenesis. J Natl Cancer Inst. 2014 106(2):djt369. doi: 10.1093/jnci/djt369

[56] Carmi Y. et al. The role of IL-1β in the early tumor cell-induced angiogenic response. J Immunol. 2013;190(7):3500–3509. doi: 10.4049/jimmunol.1202769.

[57] Xiao Q. et al. Lysyl oxidase, extracellular matrix remodeling and cancer metastasis. Cancer Microenviron. 2012 5(3):261–273. doi: 10.1007/s12307-012-0105-z

[58] Subramaniam K.S. et al. Cancer-associated fibroblasts promote endometrial cancer growth via activation of interleukin-6/STAT-3/c-Myc pathway. Am J Cancer Res. 2016;6(2):200–213.

[59] Avgustinova A. et al. Tumour cell-derived Wnt7a recruits and activates fibroblasts to promote tumour aggressiveness. Nat Commun. 2016 18(7):10305. doi: 10.1038/ncomms10305.

[60] Boire A. et al. PAR1 is a matrix metalloprotease-1 receptor that promotes invasion and tumorigenesis of breast cancer cells. Cell. 2005 120(303–313):66.

[61] Kessenbrock K. et al. Matrix metalloproteinases: regulators of the tumor microenvironment. Cell. 2010;141:52–67. doi: 10.1016/j.cell.2010.03.015.

[62] Comito G. et al. Cancer-associated fibroblasts and M2-polarized macrophages synergize during prostate carcinoma progression. Oncogene. 2014;33(19):2423–2431. doi: 10.1038/onc.2013.191.

[63] Dienz O. et al. The effects of IL-6 on CD4 T cell responses. Clin Immunol. 2009;130(1):27–33. doi: 10.1016/j.clim.2008.08.018.

[64] Öhlund D. et al. Fibroblast heterogeneity in the cancer wound. J Exp Med. 2014;211(8):1503–1523. doi: 10.1084/jem.20140692.

[65] Kojima Y. et al. TGF-beta and stromal cell-derived factor-1 (SDF-1) signaling drives the evolution of tumor-promoting mammary stromal myofibroblasts. Proc Natl Acad Sci USA. 2010;107(46):20009–20014. doi: 10.1073/pnas.1013805107.

[66] Nguyen L.V. et al. Cancer stem cells: an evolving concept. Nat Rev Cancer. 2012;12(2):133–143.

[67] Kim J.H. et al. Roles of Wnt target genes in the journey of cancer stem cells. Int J Mol Sci. 2017;18(8):1604. doi: 10.3390/ijms18081604.

[68] Borovski T. et al. Cancer stem cell niche: the place to be. Cancer Res. 2011;71(3):634–639. doi: 10.1158/0008-5472.CAN-10-3220.

[69] Shibue T. et al. EMT, CSCs, and drug resistance: the mechanistic link and clinical implications. Nat Rev Clin Oncol. 2017;14(10):611–629. doi: 10.1038/nrclinonc.2017.44.

[70] Dallas N.A. et al. Chemoresistant colorectal cancer cells, the cancer stem cell phenotype, and increased sensitivity to insulin-like growth factor-I receptor inhibition. Cancer Res. 2009 69(5):1951–1957. doi: 10.1158/0008-5472.CAN-08-2023.

[71] Serakinci N. et al. Role of mesenchymal stem cells in cancer development and their use in cancer therapy. Adv Exp Med Biol. 2018;1083:45-62. doi: 10.1007/5584_2017_64.

[72] Cillo A. et al. Immune landscape of viral-and carcinogen-driven head and neck cancer. Immunity. 2020 52(1): 183–199.e9. doi: 10.1016/j.immuni.2019.11.014

[73] Curry J.M. et al. Tumor microenvironment in head and neck squamous cell carcinoma. Semin Oncol. 2014 41(2):217-34. doi: 10.1053/j.seminoncol.2014.03.003.

[74] Koontongkaew, S. The tumor microenvironment contribution to development, growth, invasion and metastasis of head and neck squamous cell carcinomas. J Cancer. 2013; 4(1): 66–83. doi: 10.7150/jca.5112

[75] Senovilla, L. et al. Trial watch: prognostic and predictive value of the immune infiltrate in cancer. Oncoimmunology. 2012 1(8):1323-1343. doi: 10.4161/onci.22009.

[76] Fridman, W. et al. The immune contexture in human tumours: impact on clinical outcome. Nat Rev Cancer. 2012 12(4):298-306. doi: 10.1038/nrc3245.

[77] Sasidharan Nair, V. et al. Immune checkpoint inhibitors in cancer therapy: a focus on T-regulatory cells. Immunol Cell Biol. 2018 96(1):21-33. doi: 10.1111/imcb.1003.

[78] Sionov, R. et al. The multifaceted roles neutrophils play in the tumor microenvironment. Cancer Microenviron. 2015 8(3):125-58. doi: 10.1007/s12307-014-0147-5.

[79] Jaillon, S. et al. Neutrophil diversity and plasticity in tumour progression and therapy. Nat Rev Cancer. 2020 20(9):485-503. doi: 10.1038/s41568-020-0281-y.

[80] Shaul, M. et al. Tumour-associated neutrophils in patients with cancer. Nat Rev Clin Oncol. 2019 16(10):601-620. doi: 10.1038/s41571-019-0222-4.

[81] Umansky, V. et al. The role of myeloid-derived suppressor cells (MDSC) in cancer progression. Vaccines (Basel). 2016 4(4):36. doi: 10.3390/vaccines4040036.

[82] Greene, S. et al. Inhibition of MDSC trafficking with SX-682, a CXCR1/2 inhibitor, enhances NK-cell immunotherapy in head and neck cancer models. Clin Cancer Res. 2020 26(6):1420-1431. doi: 10.1158/1078-0432.CCR-19-2625.

[83] Morvan, M. et al. NK cells and cancer: you can teach innate cells new tricks. Nat Rev Cancer. 2016 16(1):7-19. doi: 10.1038/nrc.2015.5.

[84] Mandal, R. et al. The head and neck cancer immune landscape and its immunotherapeutic implications. JCI Insight. 2016 1(17):e89829. doi: 10.1172/jci.insight.89829.

[85] Muntasell, A. et al. Targeting NK-cell checkpoints for cancer immunotherapy. Curr Opin Immunol. 2017 45:73-81. doi: 10.1016/j.coi.2017.01.003.

[86] Shi C. et al. Monocyte recruitment during infection and inflammation. Nat Rev Immunol. 2011;11:762–774.

[87] Qian B-Z. et al. CCL2 recruits inflammatory monocytes to facilitate breast-tumour metastasis. Nature. 2011 475:222–225.

[88] Hanna RN. et al. Patrolling monocytes control tumor metastasis to the lung. Science. 2015 350:985–990.

[89] Engblom C. et al. The role of myeloid cells in cancer therapies. Nat Rev Cancer. 2016;16:447–462.

[90] Ziegler-Heitbrock L. et al. Nomenclature of monocytes and dendritic cells in blood. Blood. 2010 116:e74–e80.

[91] Villani A-C. et al. Single-cell RNA-seq reveals new types of human blood dendritic cells, monocytes, and progenitors. Science. 2017 356:eaah4573.

[92] Movahedi K. et al. Different tumor microenvironments contain functionally distinct subsets of macrophages derived from Ly6C(high) monocytes. Cancer Res. 2010 70:5728–5739.

[93] Kitamura T, Doughty-Shenton D, Cassetta L, et al. Monocytes differentiate to immune suppressive precursors of metastasis-associated macrophages in mouse models of metastatic breast cancer. Front. Immunol. 2018 8:69.

[94] Chun E. et al. CCL2 promotes colorectal carcinogenesis by enhancing polymorphonuclear myeloid-derived suppressor cell population and function. Cell Rep. 2015 12:244–257.

[95] Griffith T.S. et al. Monocyte-mediated tumoricidal activity via the tumor necrosis factor–related cytokine, TRAIL. J Exp Med. 1999 189:1343–1354.

[96] Yeap W.H. et al. CD16 is indispensable for antibody-dependent cellular cytotoxicity by human monocytes. Sci Rep. 2016 6:34310.

[97] Headley M.B. et al. Visualization of immediate immune responses to pioneer metastatic cells in the lung. Nature. 2016 531:513–517.

[98] Chao M.P. et al. Anti-CD47 antibody synergizes with rituximab to promote phagocytosis and eradicate non-hodgkin lymphoma. Cell. 2010 142:699–713.

[99] Kubo H. et al. Primary tumors limit metastasis formation through induction of IL15-Mediated cross-talk between patrolling monocytes and NK cells. Cancer Immunol Res. 2017 5:812–820.

[100] Lu P. et al. The extracellular matrix: a dynamic niche in cancer progression. J Cell Biol. 2012 196:395–406.

[101] Porrello A. et al. Factor XIIIA—expressing inflammatory monocytes promote lung squamous cancer through fibrin cross-linking. Nat Commun. 2018 9:1988.

[102] Madsen D.H. et al. Tumor-associated macrophages derived from circulating inflammatory monocytes degrade collagen through cellular uptake. Cell Rep. 2017 21: 3662–3671.

[103] Galdiero M.R. et al. Tumor associated macrophages and neutrophils in tumor progression. J Cell Physiol 2013 228:1404–12.

[104] Ruffell B, Affara NI, Coussens LM. Differential macrophage programming in the tumor microenvironment. Trends Immunol 2012;33:119–26

[105] Evrard D. et al. Macrophages in the microenvironment of head and neck cancer: potential targets for cancer therapy. Oral Oncol. 2019 88:29-38. doi: 10.1016/j.oraloncology.2018.10.040.

[106] Wynn T.A. et al. Macrophage biology in development, homeostasis and disease. Nature 2013;496:445–55.

[107] Biswas S.K. et al. Macrophage plasticity and interaction with lymphocyte subsets: cancer as a paradigm. Nat Immunol 2010 v 11:889–96

[108] Mantovani A. et al. Tumour-associated macrophages as treatment targets in oncology. Nat Rev Clin Oncol 2017;14:399–416

[109] Kurahara H. et al. Significance of M2-polarized tumor-associated macrophage in pancreatic cancer. J Surg Res 2011;167:e211–9

[110] Hu Y. et al. Tumor-associated macrophages correlate with the clinicopathological features and poor outcomes via inducing epithelial to mesenchymal transition in oral squamous cell carcinoma. J Exp Clin Cancer Res CR 2016;35:12

[111] Heusinkveld M. et al. Identification and manipulation of tumor associated macrophages in human cancers. J Transl Med 2011 9:216

[112] Naeim F. et al. Chapter 2 - Principles of Immunophenotyping. In: Naeim F, Nagesh Rao P, Song SX, Phan RT, editors. Atlas Hematop. Second Ed.Academic Press; 2018. p. 29–56.

[113] Lyford-Pike S. et al. Evidence for a role of the PD-1:PD-L1 pathway in immune resistance of HPV-associated head and neck squamous cell carcinoma. Cancer Res 2013 73:1733–41.

[114] Cassetta L. et al. A timeline of tumour-associated macrophage biology. Nat Rev Cancer 2023 23(4):238-257.

[115]] Ojalvo, L.S., et al. High-density gene expression analysis of tumor-associated macrophages from mouse mammary tumors. Am. J. Pathol. 2009 174, 1048–1064.

[116] Yeo, E. J. et al. Myeloid WNT7b mediates the angiogenic switch and metastasis in breast cancer. Cancer Res. 2014;74, 2962–2973.

[117] Cheng, S. et al. A pan-cancer single-cell transcriptional atlas of tumor infiltrating myeloid cells. Cell 2021;184, 792–809.

[118] Park M.D. et al. Macrophages in health and disease. Cell. 2022; 185(23): 4259–4279.

[119] Esparza-Baquer A., et al. TREM-2 defends the liver against hepatocellular carcinoma through multifactorial protective mechanisms. Gut. 2021;70(7):1345-1361.

[120] Li D.K. et al. Characteristics and clinical trial results of agonistic anti-CD40 antibodies in the treatment of malignancies. Oncol. Lett. 2020;20, 176.

[121] Peyraud F. et al. CSF-1R inhibitor development: current clinical status. Curr Oncol Rep 2017 19:70.

[122] Junttila M.R. et al. Influence of tumour micro-environment heterogeneity on therapeutic response. Nature. 2013 501(7467):346–354. doi: 10.1038/nature12626.

[123] Miserocchi G. et al. Management and potentialities of primary cancer cultures in preclinical and translational studies. J Transl Med. 2017 15(1):229. doi: 10.1186/s12967-017-1328-z.

[124] Raeber G.P. et al. Molecularly engineered PEG hydrogels: a novel model system for proteolytically mediated cell migration. Biophys J. 2005 89(2):1374–1388. doi: 10.1529/biophysj.104.050682.

[125] Pham K. et al. Isolation of pancreatic cancer cells from a patient-derived xenograft model allows for practical expansion and preserved heterogeneity in culture. Am J Pathol. 2016 186(6):1537–1546. doi: 10.1016/j.ajpath.2016.02.009.

[126] Rijal G. et al. 3D scaffolds in breast cancer research. Biomaterials. 2016 81:135–156. doi: 10.1016/j.biomaterials.2015.12.016.

[127] Egeblad M. et al. Dynamic interplay between the collagen scaffold and tumor evolution. Curr Opin Cell Biol. 2010 22(5):697–706. doi: 10.1016/j.ceb.2010.08.015.

[128] Liverani, C. et al. A biomimetic 3D model of hypoxia-driven cancer progression. Sci Rep. 2019, 9, 12263.

[129] Liverani, C. et al. Lineage-specific mechanisms and drivers of breast cancer chemoresistance revealed by 3D biomimetic culture. Mol Oncol. 2021

[130] Miserocchi G. et al. Three-dimensional collagen-based scaffold model to study the microenvironment and drug-resistance mechanisms of oropharyngeal squamous cell carcinomas. Cancer Biol Med. 2021, 18, 502-516.

[131] Sutherland R.M. et al. A multi-component radiation survival curve using an in vitro tumour model. Int J Radiat Biol Relat Stud Phys Chem Med. 1970 18(5):491–495. doi: 10.1080/09553007014551401.

[132] Thoma C.R. et al. 3D cell culture systems modeling tumor growth determinants in cancer target discovery. Adv Drug Deliv Rev. 2014 69–70:29–41. doi: 10.1016/j.addr.2014.03.001

[133] Sutherland RM. Cell and environment interactions in tumor microregions: the multicell spheroid model. Science. 1988 240(4849):177–184. doi: 10.1126/science.2451290.

[134] Peirsman, A. et al. MISpheroID: a knowledgebase and transparency tool for minimum information in spheroid identity. Sci Rep. 2016, 6, 19103. Nat Methods. 2021, 18, 1294-1303.

[135] Frankel, A.; Buckman, R.; Kerbel, R.S. Abrogation of taxol-induced G2-M arrest and apoptosis in human ovarian cancer cells grown as multicellular tumor spheroids. Cancer Res. 1997, 57, 2388-93.

[136] Dubessy C. et al. Spheroids in radiobiology and photodynamic therapy. Crit. Rev. Oncol. Hematol. 2000, 36, 179–192.

[137] Drost J. et al. Organoids in cancer research. Nat Rev Cancer 2018, 18, 407–18.

[138] Lim, YC. Et al. Cancer stem cell traits in squamospheres derived from primary head and neck squamous cell carcinomas. Oral Oncol. 2011, 47, 83-91.

[139] Driehuis, E. et al. Oral Mucosal Organoids as a Potential Platform for Personalized Cancer Therapy. Cancer Discov. 2019, 9, 852-871.

[140] Lee T.W. et al. Patient-Derived Xenograft and Organoid Models for Precision Medicine Targeting of the Tumour Microenvironment in Head and Neck Cancer. Cancers (Basel) 2020, 12, 3743.

[141] Affolter A. et al. Precision Medicine Gains Momentum: Novel 3D Models and Stem Cell-Based Approaches in Head and Neck Cancer. Front Cell Dev Biol. 2021, 8, 9:666515

[142] Leighton, J. A sponge matrix method for tissue culture; formation of organized aggregates of cells in vitro. J. Natl Cancer Inst. 12, 545–561 1951.

[143] Vescio R.A. et al. Correlation of histology and drug response of human tumors grown in native-state three-dimensional histoculture and in nude mice. Proc. Natl Acad. Sci. USA 1991, 88, 5163–5166.

[144] Majumder, B. et al. Predicting clinical response to anticancer drugs using an ex vivo platform that captures tumour heterogeneity. Nat. Commun. 2015, 6, 6169.

[145] Gormey M. et al "Reviewing the epidemiology of head and neck cancer: definitions, trends and risk factors". British Dental Journal 2022, 780–786. doi: 10.1038/s41415-022-5166-x.

[146] Elmusrati A. et al. "Tumor microenvironment and immune evasion in head and neck squamous cell carcinoma". Int J Oral Sci. 2021, 13(1):24. doi: 10.1038/s41368-021-00131-7.

[147] Wu T. et al "Tumor microenvironment and therapeutic response." Cancer Lett. 2017, 387:61-68. doi: 10.1016/j.canlet.2016.01.043.

[148] Wondergen NE, et al. "The Immune Microenvironment in Head and Neck Squamous Cell Carcinoma: on Subsets and Subsites". Curr Oncol Rep. 2020, 22(8):81. doi: 10.1007/s11912-020-00938-3.

[149] Liverani C. et al. "Investigating the Mechanobiology of Cancer Cell–ECM Interaction Through Collagen-Based 3D Scaffolds". Cell Mol Bioeng. 2017, 10(3): 223–234. doi: 10.1007/s12195-017-0483-x

[150] Becht E, et al. "Estimating the population abundance of tissue-infiltrating immune and stromal cell populations using gene expression". Genome Biol. 2016; 17: 218. doi: 10.1186/s13059-016-1070-5.

[151] Safi W. et al. “Differentiation of human CD14+ monocytes: an experimental investigation of the optimal culture medium and evidence of a lack of differentiation along the endothelial line”. Exp Mol Med. 2016, 15;48(4):e227. doi: 10.1038/emm.2016.11.

[152] Ke X. et al “Hypoxia modifies the polarization of macrophages and their inflammatory microenvironment, and inhibits malignant behavior in cancer cells”. Oncol Let. 2019, 18(6): 5871–5878.